X-ray and neutron imaging for cultural heritage: the INFN-CHNet experience

12 September 2024

Eur. Phys. J. Plus (2024) 139:635
https://doi.org/10.1140/epjp/s13360-024-05429-z

THE EUROPEAN PHYSICAL JOURNAL PLUS

Regular Article

X-ray and neutron imaging for cultural heritage: the INFN-CHNet experience

A. Mazzinghi[1,2,a], L. Castelli[2,b], C. Ruberto[1,2], S. Barone[1,2], F. García-Avello Bofías[2], A. Bombini[2], C. Czelusniak[2], N. Gelli[2], F. Giambi[1,2], M. Manetti[2], M. Massi[2], L. Sodi[2], A. Balerna[3], L. Pronti[3], M. Romani[3], M. Angelucci[3], G. Viviani[3], V. Sciarra[3], M. Cestelli Guidi[3], M. Marabotto[4,5], L. Sottili[5,6], L. Vigorelli[5,6], F. Tansella[5,6], M. Magalini[5,6], L. Guidorzi[5,6], A. Re[5,6], A. Lo Giudice[5,6], C. Ricci[5,7], F. Pozzi[5,7], G. Iorio[8,9], V. Graziani[8,9], A. Fabbri[8,9], P. Branchini[8,9], A. De Carlo[8,9,10], L. Tortora[8,9,10], M. P. Morigi[11,12], M. Bettuzzi[11,12], R. Brancaccio[11,12], M. Seracini[11,12], F. Cantini[1,2,13], F. Grazzi[2,13], G. Marcucci[14,15], M. Clemenza[14,15], D. Alloni[16,17], S. Altieri[16,18], R. Rossini[16,18], A. Salvini[16,17], O. Sans-Planell[5,6,19], D. Zafiropoulos[20], L. Sarchiapone[20], F. Arneodo[21], R. A. Torres Saavedra[1,2], M. F. Castellá[22,23], N. Mastrangelo[22,23], A. M. Morales[22,24], F. Taccetti[2], L. Giuntini[1,2]

[1] Dipartimento di Fisica e Astronomia, Università degli Studi di Firenze, via Sansone 1, 50019 Sesto Fiorentino, Florence, Italy
[2] Istituto Nazionale di Fisica Nucleare, Sezione di Firenze, via Sansone 1, 50019 Sesto Fiorentino, Florence, Italy
[3] Istituto Nazionale di Fisica Nucleare, Laboratori Nazionali di Frascati, via Enrico Fermi 54, 00044 Frascati, Rome, Italy
[4] Dipartimento di Elettronica e Telecomunicazioni, Politecnico di Torino, Corso Duca degli Abruzzi 24, 10129 Turin, Italy
[5] Istituto Nazionale di Fisica Nucleare, Sezione di Torino, via Pietro Giuria 1, 10125 Turin, Italy
[6] Dipartimento di Fisica, Università degli Studi di Torino, via Pietro Giuria 1, 10125 Turin, Italy
[7] Centro per la Conservazione ed il Restauro dei Beni Culturali "La Venaria Reale", via XX Settembre 18, 10078 Venaria Reale, Turin, Italy
[8] Istituto Nazionale di Fisica Nucleare, Sezione di Roma Tre, via della Vasca Navale 84, 00146 Rome, Italy
[9] Laboratorio Analisi Superfici Roma Tre - LASR3, via della Vasca Navale 84, 00146 Rome, Italy
[10] Dipartimento di Scienze, Università degli Studi di Roma Tre, via della Vasca Navale 84, 00146 Rome, Italy
[11] Dipartimento di Fisica e Astronomia, Università di Bologna, Viale Carlo Berti Pichat 6/2, 40127 Bologna, Italy
[12] Istituto Nazionale di Fisica Nucleare, Sezione di Bologna, Viale Carlo Berti Pichat 6/2, 40127 Bologna, Italy
[13] Consiglio Nazionale delle Ricerche, Istituto di Fisica Applicata Nello Carrara (CNR-IFAC), 50019 Sesto Fiorentino, Florence, Italy
[14] Istituto Nazionale di Fisica Nucleare, Sezione di Milano Bicocca, Piazza della Scienza, 3, 20126 Milan, Italy
[15] Dipartimento di Fisica "G. Occhialini", Università degli Studi di Milano Bicocca, Piazza della Scienza, 3, 20126 Milan, Italy
[16] Istituto Nazionale di Fisica Nucleare, Sezione di Pavia, via A. Bassi 6, 27100 Pavia, Italy
[17] Laboratorio Energia Nucleare Applicata—LENA, Università degli Studi di Pavia, via Aselli 41, 27100 Pavia, Italy
[18] Dipartimento di Fisica, Università degli Studi di Pavia, via Bassi 6, 27100 Pavia, Italy
[19] Helmholtz-Zentrum Berlin für materialien und energie gmbh, Hahn-Meitner-Platz 1, 14109 Berlin, Germany
[20] Istituto Nazionale di Fisica Nucleare, Laboratori Nazionali di Legnaro, Viale dell'Università, 2, 35020 Legnaro, Padua, Italy
[21] Division of Science, New York University Abu Dhabi, Saadiyat Island, 129188 Abu Dhabi, United Arab Emirates
[22] Centro de Estudios sobre Patrimonios y Ambiente (CEPyA), Escuela de Arte y Patrimonio, y Escuela de Hábitat y Sostenibilidad, Universidad Nacional de San Martín, Av. 25 de mayo y Francia, Buenos Aires, Argentina
[23] Consejo Nacional de Investigaciones Científicas y Técnicas (CONICET), Godoy Cruz 2290, Ciudad Autónoma de Buenos Aires, Argentina
[24] Centro Tarea, Escuela de Arte y Patrimonio, Universidad Nacional de San Martín, B. Quinquela Martín 1784, Ciudad Autónoma de Buenos Aires, Argentina

Received: 20 February 2024 / Accepted: 4 July 2024

Abstract This paper reports on the instrumentation and expertise developed within the INFN-CHNet network for X-ray and neutron imaging, which enable non-invasive identification of materials and production processes in the field of cultural heritage. INFN-CHNet is the network of the Italian National Institute of Nuclear Physics specifically dedicated to the development and application of scientific methods and technologies to cultural heritage. This article focuses on portable MA-XRF scanners, often complemented by additional techniques, PIXE imaging on a newly developed portable accelerator, X-ray radiography and tomography, exploited to their full potential also through the use of portable systems, and neutron radiography and tomography, which require large-scale facilities. In many respects, the information obtained from X-ray and neutron-based methods is complementary, facilitating a comprehensive characterisation of materials, structures, and manufacturing techniques.

[a] e-mail: anna.mazzinghi@unifi.it (corresponding author)
[b] e-mail: castelli@fi.infn.it (corresponding author)

Published online: 19 July 2024

1 Introduction

A wide range of scientific techniques based on different physical phenomena can be exploited to investigate artworks and cultural artefacts. Indeed, Heritage Science is a growing field, as it provides scientific support to the study of artworks and, in general, all natural and human production that is deemed valuable to mankind. An ever-increasing number of scientific papers to date demonstrates the successful cooperation between science and the humanities; some bibliographic references are provided in the following, though a full list is beyond the scope of this work [1–10].

In this framework, the Italian National Institute of Nuclear Physics (INFN) created its Cultural Heritage Network, known as INFN-CHNet [11], to promote the application of scientific methods and technologies developed by INFN to cultural heritage. CHNet is a multidisciplinary international infrastructure, based on the INFN laboratories' work on the development of analytical methods for the study and characterisation of cultural heritage artefacts [12], as well as on international research centres and institutions with complementary skills to those of INFN, such as conservation centres, university departments, and archaeometric associations. The structure of the network is organised into three level nodes:

1. INFN facilities throughout Italy;
2. Italian partners (conservation institutes, universities, and associations);
3. Research centres abroad.

The techniques available to CHNet can be broadly divided into dating techniques, methods for in situ analysis, and fixed laboratories for high-precision/sensitivity measurements. In addition, digital laboratories available to users are currently being developed. This is a short list of some of the INFN-CHNet scientific methods: radiocarbon dating as a dating technique, mass spectrometry, X-ray fluorescence (XRF), X-ray radiography and tomography, multispectral imaging, Raman spectroscopy, Fourier-transform infrared spectroscopy (FTIR), and ion beam analysis (IBA) as in situ and/or laboratory-based analysis.

Specifically, this paper aims at showcasing the X-ray and neutron-based techniques available within INFN-CHNet, with a special focus on macro-X-ray fluorescence (MA-XRF) coupled with other analytical techniques, particle-induced X-ray emission (PIXE) imaging, as well as X-ray and neutron radiography and tomography. One of the advantages of X-rays and neutron-based methods lies in their virtually non-invasive and non-destructive nature, a feature of primary importance when dealing with unique objects such as those related to cultural heritage studies. Also, neutron and X-ray imaging can be considered as complementary methods, as explained in more detail below. One of the differences between the two methods is that X-ray-based techniques allow the use of portable instrumentation, while those based on neutrons require the availability of large-scale facilities.

Results provided in the form of images are undoubtedly powerful and easy to read even for non-experts, a feature that widens the methods' accessibility. Indeed, images convey immediate information to conservators and scholars in the arts and humanities, facilitating the collaboration between professionals with different expertise.

Imaging can be performed either by scanning the primary beam over the sample surface and reconstructing the image pixel by pixel or by using a position-sensitive detector and obtaining a "proper" image in one shot. When adopting a scanning mode approach, spectra acquired from each point of the sample are related to the position of the beam during the scan: a datacube (X, Y, spectrum) is recorded and the images are reconstructed by plotting in false colour a slice of the spectrum (e.g. the peak area corresponding to an element in the XRF or PIXE spectrum) for each (X,Y) point (pixel). On the other hand, when employing a position-sensitive detector (commonly consisting of a discrete 2D pixel matrix) and a relatively large incident beam, an image of the irradiated area is obtained directly, typically in a significantly shorter time compared to scanning systems.

The XRF and PIXE imaging systems available to CHNet are scanning systems, in which the source and the detector are located on the same side of the object. On the other hand, radiography and tomography employ a position-sensitive detector. In these latter cases, the object is located between the source (producing a wide beam) and the detector (transmission mode). The primary beam is transmitted through the sample and the detected radiation is registered as a grey-scale image.

2 MA-XRF and complementary other techniques

Briefly, XRF uses a primary X-ray beam to prompt the emission of secondary X-rays from the target atoms. As the energies of the secondary X-rays are characteristic of each chemical element, the secondary X-ray spectrum yields insight into the sample's elemental composition, with the only exception of the lightest elements (normally XRF is limited to elements whose atomic number is greater than 10). The main advantages of XRF lie in the fact that it is a fast and multi-elemental technique; in addition, the possibility of employing X-ray tubes as a source of the primary beam enables the use of portable instrumentation, a crucial feature for in situ analysis [13–15]; furthermore, X-ray tube-based XRF is a low-cost instrumentation when compared to PIXE and Neutron imaging. On the contrary, when a synchrotron is used as a source of the primary beam, it allows for very low detection limits and very high spatial resolutions, but does not offer the possibility of in situ measurements.

The main limitation of this technique is its inability to provide data on the molecular composition and to detect organic compounds. In some cases, information regarding depth distribution can be obtained, but usually with little reliability especially for complex cultural heritage objects [16, 17].

MA-XRF is a scanning evolution of XRF that enables researchers to scan the sample surface and obtain distribution maps of the chemical elements detected. Typical map sizes range from tens to hundreds or even thousands of cm^2, depending on the type of equipment that is being used. The combined information on the elemental composition of each spot analysed and its spatial location allows one to shed light on the materials and production techniques employed.

For all these reasons, MA-XRF has been successfully applied to a great variety of objects to date [18–23], and MA-XRF scanners with different features have been developed both by scientific laboratories and private companies [24–26]. At CHNet, several MA-XRF scanners have been designed with a specific focus on Heritage Science applications, based on the expertise available at the various network nodes and within the framework of different projects, which have sometimes required combining XRF with other physical methodologies. In the following sections, the main characteristics of these instruments are described in detail.

2.1 The ultraportable MA-XRF scanner developed at INFN-Florence

This MA-XRF scanner [27] has been developed thanks to the collaboration among different nodes of the network [28]. It is a modular system, designed to be compact, lightweight, and low cost. Its mechanical parts are custom-designed (many of them 3D-printed) and controlled via open software, allowing for a complete customisation and continuous updating of the system to meet a variety of requirements that are specific to the cultural heritage field. Moreover, the use of a low-power X-ray tube and of a 4-mm-thick additional brass shielding make it a radio-safe system.

The scanner, which absorbs less than 100 W, can also be battery powered, which is a notable advantage for in situ campaigns, as those in archaeological fields with no power supply available.

All these features make this equipment accessible to a broader range of users, when compared to commercial instruments, and is suitable to be replicated in other nodes and for educational activities.

The main components of this instrument are the following:

- X-ray tube: a compact MAGNUM® by Moxtek, 40 kV maximum voltage, 0.1 mA maximum anode current. A set of eight collimators with diameters between 0.3 and 1 mm can be mounted on the tube head;
- Detection system: Amptek XR100 SDD, 25 mm^2 effective active area, 500 μm thickness, connected to a PA-210 preamplifier, in the customisable OEM configuration (heat-sinking through a home-built board; power supplies, shaping amplifier and MCA through a CAEN DT5780 digitiser);
- Autofocus system: a telemeter (Keyence IA-100) connected to a linear stage (Z-axis) to keep the sample–instrument distance constant;
- Camera to control the measuring area;
- Motion system: three linear stages by Physik Instrumente typically allowing for a maximum scanned area (XY plane) of 300×300 mm^2 (though it can be extended up to 600×400 mm^2), with a range along the focus direction (Z-axis) of 50 mm.

Motor controllers, digitiser, power supplies, electronics, and auxiliary elements are placed inside a carbon fibre box, on which the motors are installed. It is also possible to use a helium flow in between the tube and detector to mitigate the effect of absorption of the low-energy X-rays (< 1 keV), thus improving the detectability of low atomic number elements.

Acquisition in scan and point modes and data analysis are carried out through in-house developed software, based on Qt [29].

The beam size can be varied by changing the brass collimator in front of the tube. The usual size of the collimated beam on the target is 1 mm, which is obtained by using a 0.8-mm collimator, yet smaller beams can be achieved through the use of smaller collimators.

Parameters that can be set by the user include pixel dimension ($\Delta X = \Delta Y$) and scanning velocity. In general, the choice of parameters depends on the type of objects and materials. Below, typical values for two different applications are reported:

Oil on canvas/panel: velocity 10 mm/s, $\Delta X = \Delta Y = 1$ mm, acquisition time 2.5 h for 300×300 mm^2.

Ink on paper: velocity 0.5 mm/s, $\Delta X = \Delta Y = 0.25$ mm, 30 min for 10×17 mm^2.

This device has been successfully used on different kinds of artefacts (Fig. 1) [30–34].

As an example, the MA-XRF map of lead acquired on a painting by Andrea del Verrocchio, San Girolamo, from Palazzo Pitti collection in Florence is reported in Fig. 2. This map shows the use of lead white to build the volumes of the figure's face, used especially for the highlights and the white hair.

Currently, replicas of the Florence scanner are present in the following network nodes: INFN-Turin; INFN-National Laboratories of Legnaro (LNL) and INFN-Frascati (LNF); Universidad de San Martín, Buenos Aires, Argentina; New York University of Abu Dhabi (NYUAD), United Arab Emirates.

Some of them are true replicas, others have slightly different features, depending on the needs of the node.

2.1.1 The system developed at New York University Abu Dhabi

The system in use at NYUAD was initially developed as a close replica of the Florence version back in 2016. Over the years, as our research group acquired more experience with the XRF technique and equipment, new lines of research were pursued in terms of instrumental advances. In particular, the NYUAD version of the MA-XRF instrument utilises two independent detectors for

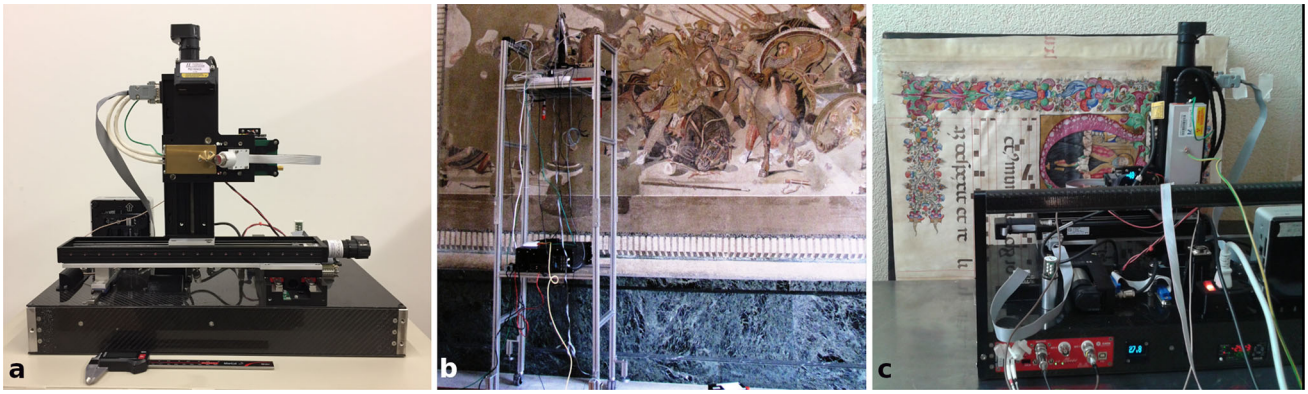

Fig. 1 **a** CHNet MA-XRF system developed in Florence. **b** Analysis of the Battle of Issus Mosaic at the Museo Archeologico Nazionale di Napoli, Italy, during a campaign funded by IPERION CH.it. **c** Analysis of manuscripts in San Giorgio Maggiore in Venice, during a campaign funded by the MINIARE project

Fig. 2 Painting by Andrea del Verrocchio, San Girolamo (ca. 1460), mixed media on paper glued on board, 40.5 × 27 cm, conserved in the Galleria Palatina in Florence. Superimposed to the painting, the MA-XRF map of lead (white corresponds to the maximum number of PbLa X-rays detected in the area, while black to the minimum)

the X-rays emitted in the interaction between the beam and the material under analysis. The development of this bi-detector setup prompted the integration with specific software, mechanics (support), and electronics for the management, implementation, and handling of two detectors and for the acquisition of spectroscopic signals that are synchronised and coherent with each other.

The choice to develop a bi-detector setup was motivated by the materials encountered in our collaborative projects and applications. Indeed, most of the materials analysed consisted primarily of earthenware, including shards of both glazed and unglazed pottery obtained from either surface surveys in archaeological regions, or rescued from shipwrecks. Given the relevant number of requests related to pottery shards, an efficient and fast detection of such low atomic number materials became of key interest to our research

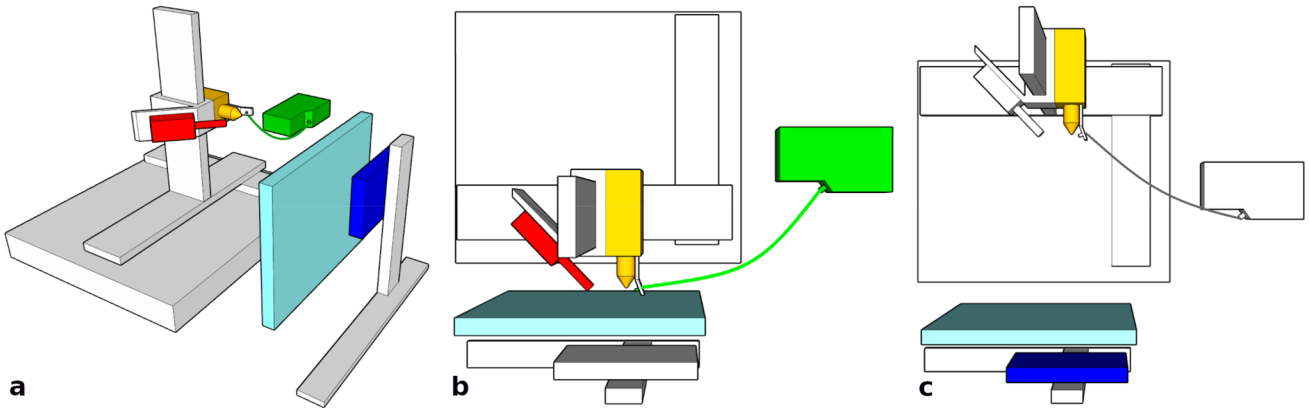

Fig. 3 **a** CHNet MA-XRF system developed in Turin. The main components are highlighted with different colours as follows: X-ray tube (yellow), sample (cyan), XRF detector (red), XRL detector (green), and DR detector (blue). **b** Instrument configuration for XRF and XRL. **c** Instrument configuration for DR

team. In other words, we aimed to increase as much as possible the amount of collected statistics during the typical duration of a scan.

With these considerations in mind, the NYUAD instrument was designed to match the technical specifications of the Florence system, already described in Sect. 2.1, apart from the hardware features listed in the following:

- Detection system: two compact Amptek AXR-SDD detectors with an effective active area of 25 mm^2 and thickness of 500 μm, inside a standard TO-8 package, each connected to a PA-210 preamplifier;
- Data acquisition system: a digitiser (CAEN DT5780) converting the analogue signal from the preamplification stage of each detector into a digital signal. The digitiser then applies a digital shaping algorithm, which enables to bin the pulse amplitudes into a single histogram for each detector. After calibration, this histogram can be interpreted as an X-ray energy spectrum;
- Helium flow system: a microcontroller (STM32F0) to adjust the helium flow to the instrument head, used to mitigate the effect of absorption of the low-energy X-rays (<1 keV), thus increasing the signal-to-noise ratio for low atomic number elements;
- Motion system: three linear stages by Physik Instrumente, allowing typically for a maximum scanned area (XY plane) of 200×200 mm^2, with a focus distance (Z-axis) of 50 mm.

Additionally, the measurement head and the scanning system are enclosed within a lead-glass box interlocked with the controller of the X-ray tube to meet the local requirements for radio-safety (if the glass window is opened, the X-ray tube is automatically powered off).

2.1.2 The system developed at INFN-Turin

A modified version of the MA-XRF scanner was developed by researchers of the INFN-CHNet Turin node (Fig. 3). This apparatus, too, is lightweight and compact, with the additional possibility to perform multiple X-ray-based techniques using the same tunable X-ray source. The techniques currently available within this system are MA-XRF, X-ray-induced luminescence (XRL), and digital radiography (DR).

The main differences in the hardware compared to the MA-XRF Florence scanner described in Sect. 2.1 are related to the possibility of performing DR. Indeed, the instrument-object distance required in radiography is higher with respect to XRF, and an X-ray tube with a slightly higher voltage and power was necessary, given the mean thickness of the artworks examined. The Z-axis, used in the original instrument to keep the distance between the measuring head and the sample constant, is here used also to increase the sample to X-ray tube distance, to obtain a wider beam, able to invest the whole area of the sample that can be imaged by the radiography detector (at the maximum distance of about 250 mm from the artwork and without collimators, an area of about 20 cm in diameter is illuminated by the X-ray beam). For this task, the Z distance needs to be varied over a significantly larger distance with respect to that needed in the Florence scanner. With this instrument, it is possible to obtain the radiography and XRF map of the same area of an object simultaneously, without moving the system.

In addition, a detection system for XRL was added.

These new features have prompted changes in the hardware, always paying attention to maintaining the whole system compact and lightweight so as not to compromise its portability.

In light of these considerations, the Turin instrument was also developed with the same technical features as the Florence equipment, except for the items described below:

- X-Ray tube: Moxtek 12 W MAGPRO [35], 60 kV maximum voltage, 1 mA maximum anode current;
- Motion System: a linear stage by Physik Instrumente with a travel range of 200 mm in the Z-axis;

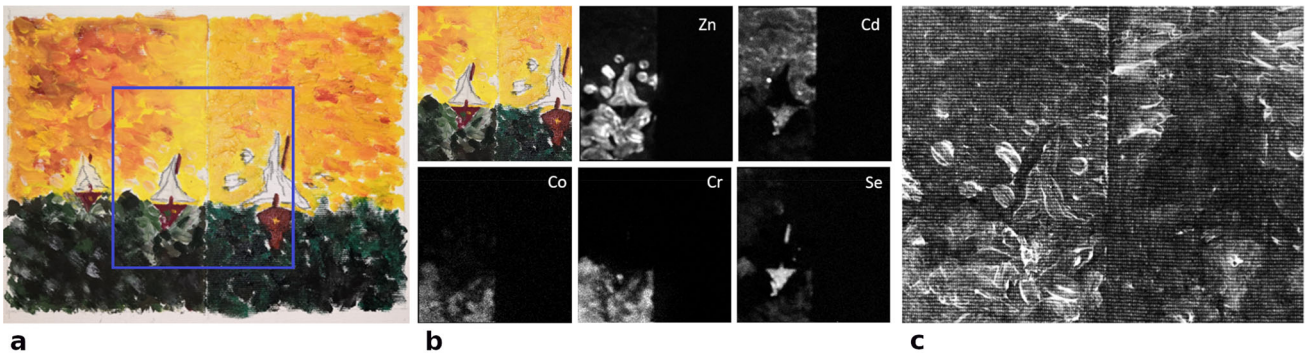

Fig. 4 **a** Visible image of a mock-up painting on canvas. **b** MA-XRF elemental maps of an area of 100 × 100 mm^2, acquired using the following parameters: X-ray tube 50 kV and 200 μA, instrument-object distance 10 mm, collimator 1 mm, scanning speed 5 mm/s, pixel size 500 μm. **c** Radiography, acquired using the following parameters: X-ray tube 40 kV and 100 μA, source-detector distance 185 mm, acquisition time 1 s

Fig. 5 Left, visible image of a wooden sculpture from Palazzo Granieri. Right, radiograph of the same object, acquired using the following parameters: X-ray tube 60 kV and 150 μA, source-detector distance 600 mm, acquisition time 7 s

- XRL detection system: UV-74 collimating lens coupled with the QEPro spectrometer by OceanOptics [36] (wavelength range 250–1100 nm);
- DR detection system: Shad-o-Box HS model 6 K by Teledyne [37]. It is a 2D CMOS detector with an active area of 11.4 cm × 14.6 cm, a pixel size of 49.5 μm, and maximum integration time of 65 s.

The device has been tested on various types of objects and materials [38, 39]. Radiography and elemental maps were acquired for a mock-up painting on canvas (Fig. 4). The elemental maps revealed a different composition on the two sides of the work. In particular, the left part is characterised by the presence of multiple elements, whereas on the right side, no medium–high atomic number element was detected, such as those characteristics of mineral pigments, attesting the use of organic materials such as lake pigments. The difference between the two sides is also highlighted in DR.

Thanks to its versatility, the instrument also enables the radiography of three-dimensional objects. As an example, Fig. 5 shows the radiograph of a wooden sculpture in the collection of "Gabinetto verso la via" at Palazzo Granieri (Turin, Italy). This object was produced around the mid-eighteenth century by the workshop of Pietro Massa, who specialised in the production of Chinese-style artefacts [40].

The XRL detection system was also tested on two lapis lazuli rocks, one from Chile and one from Afghanistan, to study the minerals' luminescence signals, which serve as markers to identify the rocks' provenance [41, 42]. The samples' signal was collected with a UV-74 lens and sent to the spectrometer via the QP1000-2-UV–VIS optical fibre, yielding the results shown in Fig. 6a, b. As observed in the images, the spectrum for the Chilean rock shows a double band at 560 nm and 620 nm, while one band only, located at 585 nm, can be detected for the Afghan mineral. These results suggest the presence of wollastonite ($CaSiO_3$) in the Chilean samples and of diopside ($CaMgSi_2O_6$) in the Afghanistan specimens, as also obtained in a previous study (Fig. 6c) [43].

2.1.3 The MA-XRF system coupled with FTIR and UV techniques at INFN-LNF

The coupling of XRF with other imaging techniques is crucial to integrate complementary pieces of information on organic compounds and on their molecular composition. For this reason, recent technological advances have been focused on the development of multi-sensor scanning systems operating in an extended spectral range [44, 45] and coupled with data fusion approaches to obtain multi-level information on the artwork analysed [46, 47].

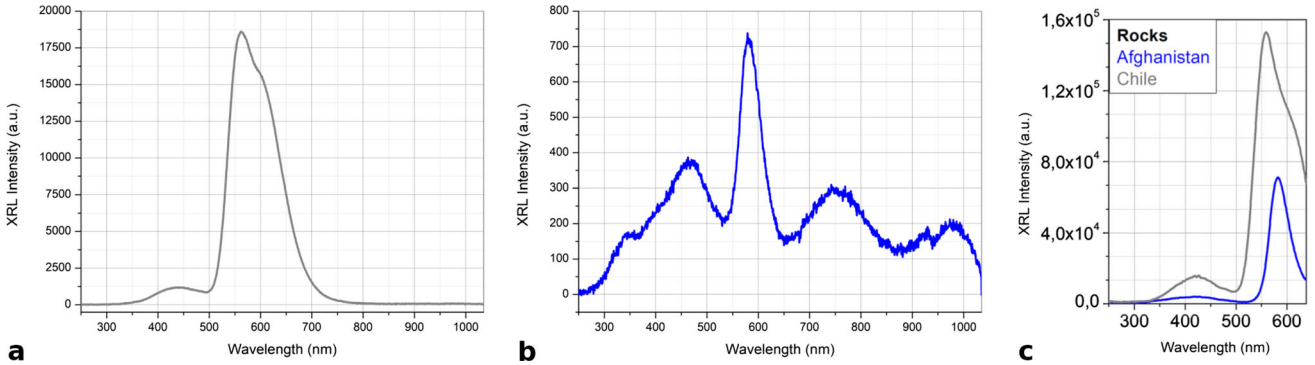

Fig. 6 XRL spectra for Chilean (**a**) and Afghan (**b**) lapis lazuli, acquired using the following parameters: X-ray tube 20 kV and 600 μA; **c** luminescence spectra for Chilean and Afghan samples from a previous study [42] acquired using the following parameters: X-ray tube 20 kV and 600 μA

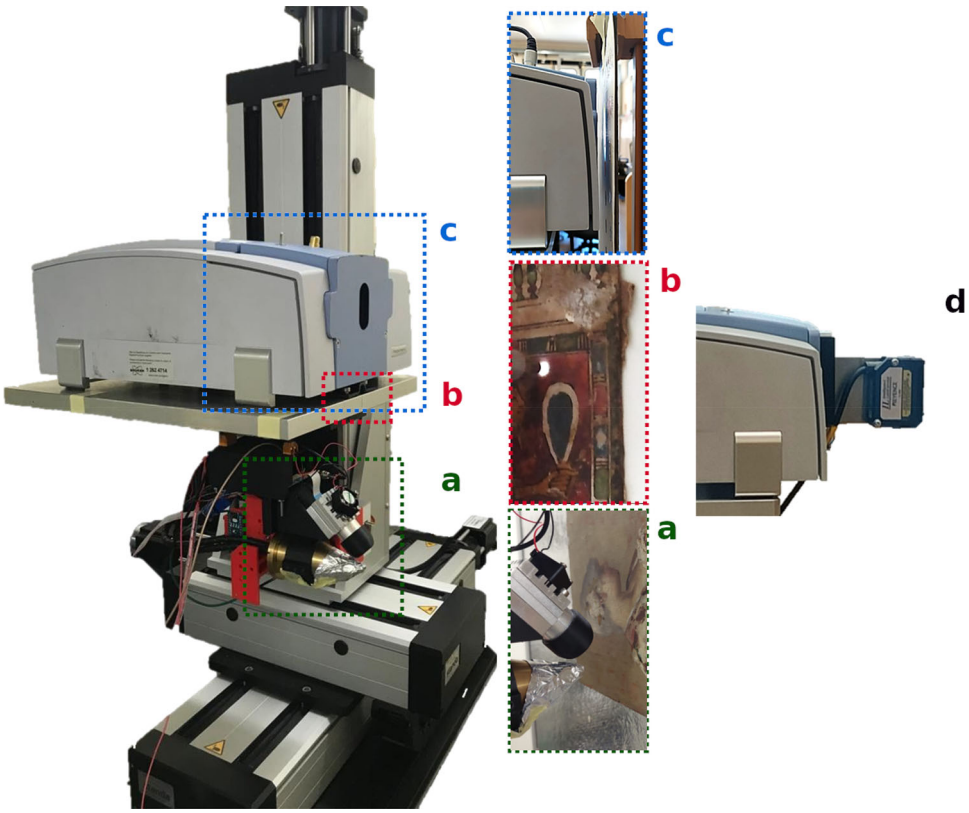

Fig. 7 Multi-sensor scanning system with its multiple components: **a** XRF, **b** UV-induced fluorescence, **c** FTIR, and **d** position sensor mounted on the FTIR spectrometer

An integrated scanning system able to perform measurements using different spectroscopic techniques (XRF, UV-induced fluorescence spectroscopy and FTIR spectroscopy in reflection mode) has been developed at the DAFNE-Light laboratory of INFN-Frascati National Laboratory (LNF) within the ARTEMISIA (ARTificial intelligence Extended-Multispectral Imaging Scanner for In situ Artwork analysis) project funded by the Lazio Region Technological District of Cultural Heritage (DTC).

The scanning system is composed by a 3-axes motorised translator (Standa), which enables data collection in the X–Y directions by focusing the probing beam onto the analysed surface (in the Z direction, as illustrated in Fig. 7). The maximum dimension of the recorded maps is 200×200 mm^2.

The composite instrument, shown in Fig. 7, yields data on the elemental and molecular composition of the same area of a given object. In detail, the scanning system includes the following components:

a. XRF: an X-ray source and a silicon drift detector (SDD) with preamplifier and cooling system for the XRF measurements;
b. LED-UV: the optical probe for the LED-UV-induced fluorescence measurements;
c. FTIR: a spectrometer for the FTIR measurements;

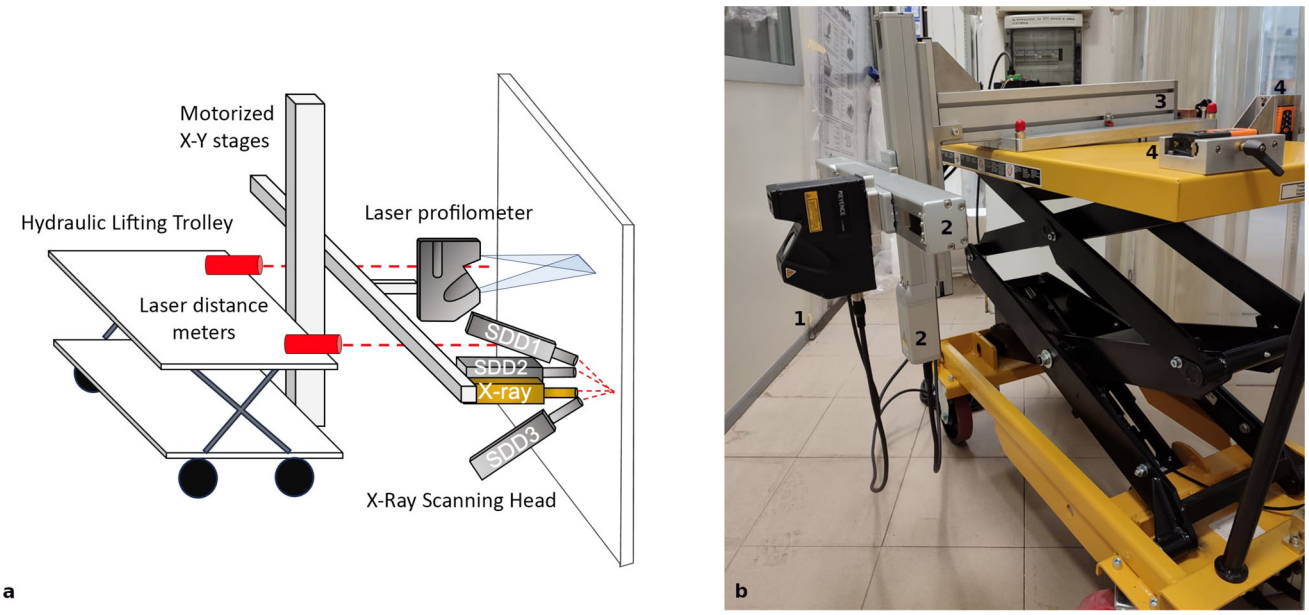

Fig. 8 **a** Schematic representation of the X-ray scanning head and the profilometer sensor head. **b** Transportable scanning system with its components: (1) Laser profilometer; (2) motorised X–Y stages; (3) inclination adaptor; (4) laser distance metres

d. A position-sensitive sensor (IL-65, Keyence), used to map and record the X, Y, and Z positions of the area to be analysed before the acquisition. These recorded positions are then employed for the three techniques (X-rays, UV, and IR), as the distance among the three measuring heads is known and fixed.

All the other components (i.e. electronics, UV source, UV–Vis spectrometer, etc.) are located on a working table.

The spectral acquisitions are synchronised with the scanner movements by means of a LabVIEW software developed in-house, whereas the images are reconstructed through a dedicated software (ARTEMISIA software) developed by X-Team Software Solutions.

The setup for each spectroscopic technique is briefly described below:

- XRF: X-ray tube and detection system as in the Florence version (see Sect. 2.1). The beam spot size is approximately 1 mm;
- LED-UV: LED-UV source, centred at 280 nm (Ocean Insight), and a UV–Vis spectrometer (FLAME Ocean Insight). The spectrometer is equipped with a 600 lines/mm diffraction grating, blazed at 300 nm, covering a 200–850 nm spectral range, and a linear silicon charge coupled device (CCD) array detector. The spectral resolution is 1.5 nm. An optical probe excites and collects light in a position perpendicular to the sample and two optical fibres are connected to the UV source and spectrometer, respectively. The beam spot size is approximately 1 mm;
- FTIR: a commercial Bruker Alpha FTIR spectrometer, equipped with a reflection module (20°/20° geometry) and a coaxial digital camera. The camera acquires one image for each acquisition point, which allows assigning spectra to specific spots on the map. The lateral resolution is approximately 1.5 mm, and the spectral range is 7000–350 cm^{-1}.

2.2 The combined MA-XRF and profilometry scanner at INFN-Roma Tre

An integrated system for chemical and morphological analysis is being developed in the framework of the PERSEPOLY (Protecting hEritage by x-Ray SpEctroscopy and PrOfiLometrY) project, conceived as a continuation of the Mu.S.A. (Multi-Channel Scanner for Artworks) project, which was conducted from 2019 to 2021, which was devoted to developing a MA-XRF scanning system [12, 48–51]. A laser profilometry device was subsequently added (Fig. 8a), further enhancing the overall investigative capabilities of the system.

Integrating non-destructive and non-invasive techniques into the available MA-XRF device can provide precious information complementary to the elemental composition especially for the analysis of paintings. Laser profilometry offers several advantages for addressing diagnostic needs in the study of cultural heritage. When scanning semi-flat surfaces of different composition, the system's lateral resolution of about ten microns allows for very precise and reproducible localisation of the features of interest, such as hidden details, details related to the production techniques, or surface defects due to degradation processes [52, 53]. Thanks to the micron-level vertical resolution (along the Z-axis perpendicular to the painting plane), the system enables the study of brushstrokes, whose usual size is 20–30 microns in height and above 200 microns in width. Moreover, laser profilometry delivers quantitative data, enabling the creation of topographical maps and 3D representations, along with conducting calculations of surface roughness and statistical studies [54]. Alternatively, these data can be processed towards a format accessible also to conservators and art

historians, displayed as a simulated raking light image, coloured scale topographic map, for more immediate interpretation of the surface features, from the perspective of artistic gesture. These formats can be easily handled by any image viewer (i.e. GIMP and Photoshop) and 3D viewer (i.e. MeshLab and Gwyddion). Finally, the possibility of repeating surveys at different times facilitates the detection of changes in the object's shape and variations in surface layer thickness during cleaning processes [55, 56].

The profilometry scanning system contains the following components:

- Profilometer: a high-resolution laser profilometer by Keyence (Controller Model: LJ-X8000A; Head Model: LJ-X8080). A laser line ($\lambda = 405$ nm) measuring 39 mm $\times$ 72 μm is projected on the object, and the sampling rate can vary from a minimum of 10 Hz to a maximum of 1 kHz. The CMOS captures the reflected light, leveraging it to generate a detailed surface profile. With a working distance of 72 mm and a measurement range spanning $\pm$20.5 mm, the instrument delivers height data with a lateral resolution of 12.5 μm [57];
- Motion system: two motorised linear axes (X, Y) by IAI Corporation (Model: RCP6-SA6C-WA-42P-3-300-P3-R03), enabling a maximum scanning area in the XY plane of 300 300 mm^2 [58];
- Hydraulic Lifting Trolley: The entire setup has been transferred on a Columbus McKinnon elevating platform (Model: HF A 035-1575 DM), which can be raised up to 150 cm [59], facilitating the scanning of large-scale paintings. Additionally, it has been modified by integrating a system that enables the adjustment of the eventual inclination angle, ensuring optimal scanning conditions (Fig. 8b).

The technical specifications of the XRF system are reported elsewhere [12, 49–51]. The operational speed range of the current setup is not congruent with the capabilities of the system developed in the Mu.S.A. project. As a result, the two instruments require movement at different velocities, making consecutive runs necessary instead of simultaneous operation. The high reproducibility of the head mechanical positioning (in the range of 10 microns, less than the profilometer lateral resolution) allows for precise overlapping of the two levels of information, morphological and compositional.

As a preliminary phase, ad-hoc samples prepared with different materials and thicknesses were examined to verify the instrument's accuracy and compatibility with the MA-XRF scanner's working conditions [60, 61]. Subsequently, a panel painting titled *L'ebbrezza di Noè* (measuring 170 cm $\times$ 120 cm), belonging to the Gallerie Nazionali di Arte Antica, Rome, was studied (Fig. 9a). Three significant details of the work are shown in Fig. 9, along with the surface morphology of three areas. In Fig. 9c, in the corresponding 3D model, the thicker brushstrokes of the highlights on the hair, eye, and facial contours are clearly visible, as they were added at the end of the creative process by applying a thick, clear paint that conveys a relief effect. The colour scale indicates a slight depression of the panel, corresponding to the forehead. Figure 9d and e shows a junction between two wooden planks of the panel, affected by paint detachments (red circle). Furthermore, the 3D model reveals warping of the two planks. Finally, Fig. 9f and g details the contours of the seal with the letters "A S", located at the bottom right corner and possibly signed by the unknown artist. The comparison also highlights an additional advantage of the profilometric survey over the autopsic one, i.e. the absence of specular reflection (in this case present on the red lateral surface of the lettering), which can hinder proper reading of the materials' morphology. Each point in Fig. 9g retains the height information and is fully legible.

The hyphenation of the two techniques proved to be highly effective in addressing a series of crucial issues for the study of cultural heritage. From a conservation point of view, it is possible to follow the evolution of degradation phenomena in paintings, such as the harmful interaction of oil media with pigments or drying additives containing metals such as Pb, Zn, Co, or Mn that may induce craquelure or the crystallisation of metallic soaps granules, with consequent eruption on the painted surface. Other instances of surface changes linked to specific elemental compositions include paint crumbling, observed for example in the case of As-based colours such as realgar, orpiment, emerald green, or efflorescence phenomena related to the release of migrating ions from pigments, as in the case of the leaching of alkali ions from the blue smalt. The technology presented herein may in the future simplify the systematisation of knowledge about the phenomenology of craquelure in specific pigment-binder formulations. Furthermore, in the context of stylistic and formal analysis of works of art, it will be possible to apply pattern recognition and classification algorithms to the paintings investigated. For example, it will be possible to identify different hands within the same painting, later conservation treatments or changes, and to evaluate a work's authenticity thanks to the reconstruction and documentation of the pictorial phases and the examination of the artist's techniques.

In summary, the integration of MA-XRF and laser profilometry is a promising approach for the study and preservation of cultural heritage. This synergistic combination contributes to addressing numerous challenges associated with degradation and understanding of the artistic practices.

3 PIXE imaging

PIXE uses a particle beam of MeV energy (most typically, a 2–3 MeV proton beam) to excite the emission of X-rays from the atoms of the target. Since the energies of these X-rays are characteristic of each chemical element, the X-ray spectrum provides the elemental composition of the sample, with the only exception of the lightest elements (normally PIXE is limited to elements whose atomic number is greater than 10). Proton beams with typical intensity ranging from a few tens of pA up to a few nA are the most common choice; they are usually produced by electrostatic accelerators with terminal voltage of some MV.

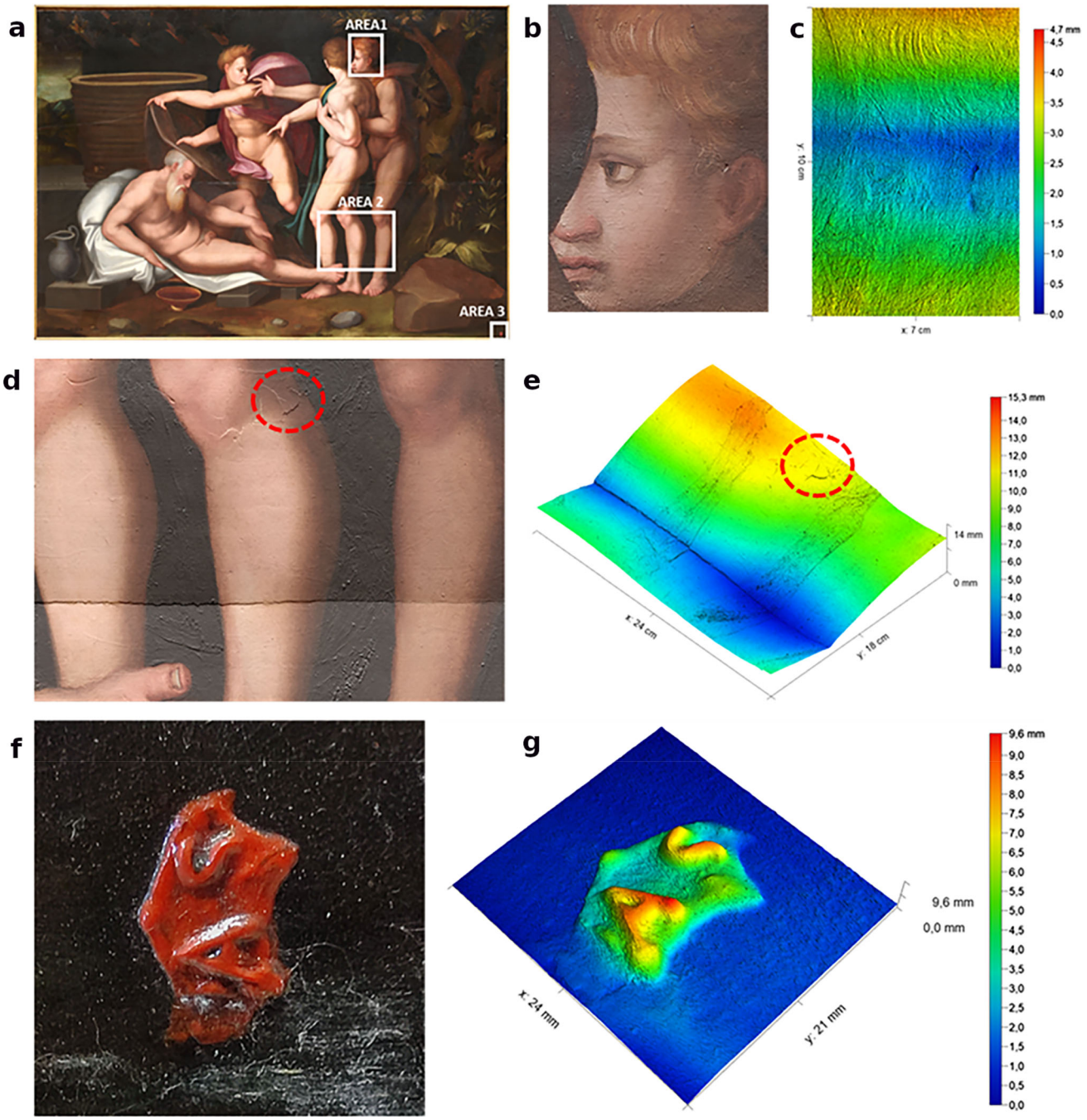

Fig. 9 **a** Visible light image of the panel painting 'L'ebbrezza di Noè', Gallerie Nazionali di Arte Antica, Roma (MiC) - Bibliotheca Hertziana, Istituto Max Planck per la storia dell'arte/Enrico Fontolan; **b** area 1, superimposition of profilometry height image to the visible light image and **c** 3D model for a documentation of the brushstrokes; **d** area 2, superimposition of profilometry height image to the visible light image and **e** 3D model for an integrated documentation of surface defects; **f** area 3, visible light image and **g** 3D model of the seal with the letters "A S"

PIXE is a multi-elemental technique that enables high sensitivity measurements (down to trace elements), also in a quantitative way, since all the physical parameters determining the X-ray yield (production cross section, beam energy loss in penetrating the target, absorption of the produced X-rays) are well known. The sample can be kept in air, thanks to external beam setups [62], and the beam current can be very low (tenths of pA are often sufficient with thick targets), preventing any damages to the object under study [63].

The possibility of tuning the proton energy, and thus the proton range, into the sample allows one to obtain information on the structure in depth; moreover, the simultaneous emission of additional radiation from the target can be exploited by complementary

techniques (for instance, PIGE, when detecting gamma rays, IL when collecting visible light, EBS/RBS, in the case of elastically backscattered particles) to integrate the wealth of information gathered in the analysis.

As already noted in the case of XRF, the main limitation of PIXE is its inability to yield information on the material's molecular composition and identity of the organic compounds. Moreover, the use of particle accelerators makes this technique typically not suitable for in situ analysis, with a few notable exceptions discussed below.

Imaging can be performed either by scanning the beam over the sample surface using electrostatic or magnetic deflectors (typically with areas up to some square mm) or by moving the sample in front of the beam, which is possible only if the artefact's size and weight allow it to be placed on a motorised frame. In the latter case, larger areas, typically of the order of tens or hundreds of cm^2, can be examined.

3.1 PIXE imaging system at the MACHINA portable accelerator

MACHINA is the first transportable particle accelerator ever built [64], developed within a project that involved INFN, the Conseil Européen pour la Recherche Nucléaire (CERN), and the Opificio delle Pietre Dure (OPD) to perform elemental analysis of objects of interest to cultural heritage.

MACHINA was designed to be installed in the OPD laboratories and moved, when needed, to museums, storages or conservation sites. With this goal in mind, this system had to meet a number of requirements, including low weight, compactness, low power consumption, low radiation impact, low cost, transportability, and ease of use.

As a whole, the accelerator system, which provides 2 MeV pulsed proton beams that can be used for PIXE and PIGE, weighs under 500 kg, occupies a space approximately 2.5 m in length (beam axis) and 1 m in width, and consumes an average power of less than 15 kW.

MACHINA consists of four main parts:

1. the radiofrequency (RF) ion source, producing a 20 keV proton beam;
2. the low energy beam transport line (LEBT), which drives the protons in ultra-high vacuum (UHV) from the source to the principal accelerating structure; it contains a focusing system (Einzel lens) and a diagnostic station equipped with a Faraday cup;
3. the radiofrequency quadrupole (RF) cavities, where the beam is bunched, focused, and accelerated from 20 keV up to 2 MeV;
4. the High-Energy Beam Transport (HEBT), another UHV line driving the protons from the RFQ cavity to the beam extraction window, which allows for the beam to be extracted from the high vacuum beamline into the atmosphere. In the HEBT, a beam focusing system (based on two permanent quadrupole magnets) and a diagnostic station, to measure beam current, position, and shape, are also present. In addition, a rotating carousel enables the introduction of aluminium foils of two different thicknesses to reduce the beam energy. In detail, beams on target of 1.5 MeV and 1 MeV can be obtained by inserting, along the beam path, aluminium foils of 9 μm and 22 μm, respectively.

The sample is placed a few millimetres after the exit nozzle. Here, a carbon fibre frame mounted on top of two precision motorised stages from Physik Instrumente (PI) allows for a maximum scanned area of 600×200 mm^2, with a maximum load of about 20 kg. The beam diameter can be adjusted from some mm to some hundreds of micrometres. Exact characterisation of this system is still in progress.

4 X-ray radiography and computed tomography

X-ray digital radiography (DR) and computed tomography (CT) are non-invasive testing techniques that use X-rays to investigate the entire volume of an object.

Differently from MA-XRF, in X-ray radiography, the object is placed between the source and the detector, and the intensity of the transmitted radiation, attenuated through the sample, is recorded as a grey-scale image. This intensity is related with physical parameters such as density and atomic number of the object analysed, allowing researchers to reveal internal details and providing morphological and physical data on its inner structure. The analysis can shed light on construction techniques, conservation state, and materials distribution [65].

CT consists in acquiring a series of radiographies at different angles of the object with respect to the source-detector system; information can be obtained as 2D cross-section images or 3D full-volume images, enabling the inspection and classification of the structure of the object. Additionally, processing tomographic data can result in a 3D numerical model of the sample, suitable for virtual reality applications or digital archive storage.

X-ray CT is limited by the objects' material composition and size. Large metal works require high energy X-rays, which involves issues related, for instance, to radio-safety and transportability of the dedicated instrumentation. Moreover, X-rays typically yield poor contrast for organic materials, especially when they are embedded into objects with higher density.

The technique was first applied to cultural heritage analysis using medical CT scanners with hospital permission. However, medical CT scanners only produce accurate results when analysing samples whose size and density is similar to that of the human body. Unfortunately, with the notable exception of mummified individuals, this requirement is rarely met in the field of cultural

heritage research, where artefacts exhibit different sizes and compositions. For maximum flexibility in terms of portability and object dimensions, custom instrumentation is designed and developed with unbonded, independent components: source, object sample stage, and detector. This configuration allows for 360° projections to be acquired by rotating the objects, as opposed to medical systems. This involves using two orthogonal translation axes to move the detector on an X–Y plane and Z-translation to move the source, so that the tile-scanning technique can be used to perform CT of artworks larger than the detector dimensions. Over the years, INFN-CHNet researchers developed multiple acquisition systems for DR and X-ray CT [66, 67], starting from instruments tailored for large objects up to a few metres in size and high-resolution micro-tomography for small artefacts (with a voxel size of a few microns) [68–71].

4.1 CT systems at INFN-Bologna

The CHNet node in Bologna was born from the synergy between the University of Bologna, Department of Physics and Astronomy (DIFA), and the INFN, Bologna division. Over the past decades, several CT systems were developed, four of which are fully operational at the present moment. They are located in three different X-ray laboratories, two of which are based at DIFA in Bologna and one in Ravenna.

Of these four systems, two are fixed (a micro-CT apparatus and a scanner for large-scale objects) and two are mobile (a medium-sized scanner and a system for large objects). The two mobile systems described in the following are the most unique pieces of equipment of the CHNet Bologna node. Decades of collaborative work with cultural heritage institutions such as museums and conservation centres have highlighted a widespread need for on-site analytical capabilities. To meet this requirement, over several years and through a series of subsequent adjustments, the team developed two additional setups for mobile X-ray CT, covering both medium (a few tens of centimetres) and large (up to 1.5 m) dimensional scales, respectively. Both systems feature flat-panel detectors, which are well suited for movable apparatuses thanks to their compactness. A combination of commercially available and custom-designed mechanics completed the scanners' structure.

A description of the four X-ray CT scanners is reported in the following, with a special focus on the two mobile systems.

4.1.1 Fixed CT system for large-scale objects in Ravenna

Formerly developed for on-site campaigns, the system was modified and eventually located in the Ravenna laboratory. The detector is a scintillator-mirror-CCD camera mounted into a light-proof box. The components, updated multiple times over the years, are now the following:

- X-ray tube: COMET Yxlon EVO200D (200 kV, 6 mA);
- Detection system: Apogee Alta U9000 CCD camera plus mirror and caesium iodide scintillating screen;
- Motion system:
  - 3 m travel range horizontal high-load motorised linear stage;
  - 80 cm travel range motorised vertical lifter;
  - Newport RV160CC high-load rotation stage.

The system has been fully functional as a stationary CT scanner for large-scale objects since 2008. With a field of view of 45 cm × 45 cm that can be extended mechanically, this equipment is currently mainly used for teaching purposes.

4.1.2 Fixed micro-CT system in Bologna

The micro-CT system currently operating at the University of Bologna's Department of Physics and Astronomy was developed based on a high-resolution CCD camera.

The main components of the system are as follows:

- X-ray tube:
  - low power and compact microfocus tube Thermo-Kevex PXS10-65W 130 kV;
  - BOSELLO XRG120IT Industrial type X-ray tube 120 kV—7 mA;
- Detection system: Photonic Science VHR1:1 CCD camera (4000 × 2600—9 μm pixel) with GOS scintillator;
- Motion system:
  - Physik Instrumente M-037 micrometric rotating stage;
  - Physik Instrumente M-042 tip/tilt precision alignment goniometers;
  - Physik Instrumente M-415 vertical translation axis for sample adjustment.

This system works for high-resolution sample scanning down to 4.5 μm voxel at maximum resolution, while the typical voxel size used is between 9 and 12 μm. The field of view of the Photonics Science CCD camera sensor is 36 mm × 23.4 mm, becoming

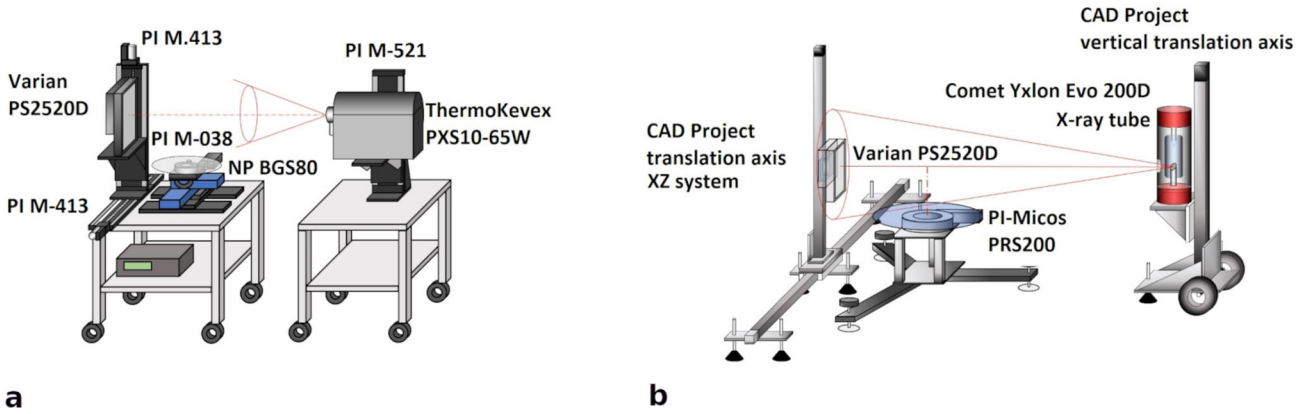

Fig. 10 Schematic illustration of the mobile systems of the CHNet Bologna node (INFN-DIFA): **a** medium-size mobile system for small objects (flat-panel motorised stage length 30 cm for both horizontal and vertical axis), and **b** large-size mobile system for large objects (flat-panel motorised stage length 1.5 m for both horizontal and vertical axis)

9 mm × 5.85 mm at the maximum resolution available with 4.5 μm voxel size. For that reason, the system is suitable for the analysis of samples of quite small dimensions (< 3 cm).

4.1.3 Medium-size CT mobile system for small objects

The first mobile system setup (Fig. 10a) consists of a couple of wheel tables, on top of which the components are mounted. The first table is dedicated to the flat-panel detector and rotation-tip/tilt sample manipulator block, while the second table holds the compact X-ray tube and a vertical translation axis for height adjustment.

Listed below are the system's main components:

- X-ray tube:
  - COMET Yxlon EVO200D (200 kV, 6 mA) for high energy scanning;
  - Thermo-Kevex PXS10-65W compact low-power X-ray tube for high-resolution scanning;
- Detection system: Varian PaxScan 2520D medium-size flat-panel detector with 1536 × 1920 image size and 127 μm pixel;
- Motion system:
  - Physik Instrumente M-413 30-cm travel range motorised stages XZ detector translation system;
  - Physik Instrumente M-038 precision rotary stage;
  - Newport BGS80 precision goniometers pair;
  - Physik Instrumente M-521 20 cm travel range vertical translation stage (for X-ray tube).

The flat-panel field of view, thus measuring about 20 cm × 24 cm, can be extended to a 30-cm travel length each by means of vertical and horizontal translation axes. The extended field of view reaches roughly an overall dimension of 50 cm × 54 cm. Extended field of view CT is possible by applying the tile-scanning method, which relies on a complete rotation of the sample over 360 degrees with related projection acquisition on a number of shifted overlapping detector positions belonging to a previously established grid. In the present working configuration, our system allows a maximum grid of 3 × 3 detector positions. Anyway, because of magnification, the maximum physical size of the object to scan is 40 cm.

With the microfocus X-ray tube, the mobile system shows good high-resolution capabilities, reaching a voxel size of around 30 μm, while normal operations entail a voxel size of 110 μm. The choice of experimental parameters depends, of course, on the sample size and resolution requirements, and will affect the overall field of view achieved.

Easy to transport and set up, this medium-size mobile system has been used in several on-site measurement campaigns across Italy. The ordinary way of transportation is through a van, although the components (without the tables) can also be shipped and reassembled on-site. This is what was done, for instance, on the occasion of some analytical campaigns on the main Italian islands (Sicily and Sardinia) or in remote locations (Calabria) [72].

4.1.4 Large-size CT mobile system for large objects

The second mobile system is based on a custom mechanics assembly, a detector, a rotation stage, and an X-ray tube (Fig. 10b).

A list of the system's main components is reported below:

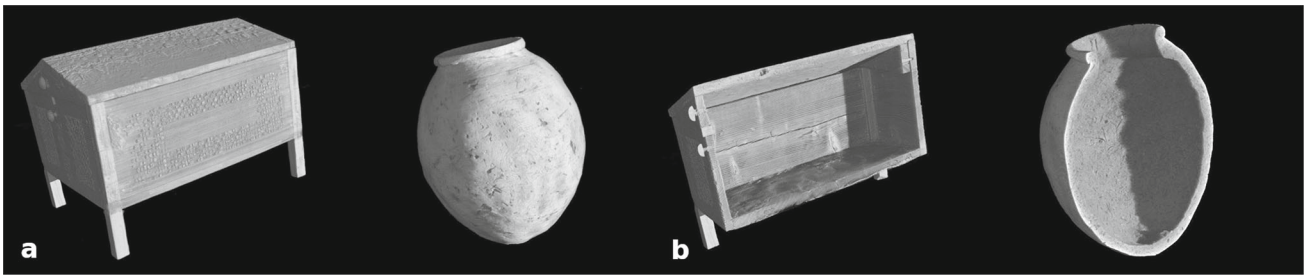

Fig. 11 3D rendering of two CT scanning campaigns performed at the Museo Egizio in Turin: **a** a wooden box from the Tomb of Kha and Merit; **b** a small vase from the Eliopolis material currently under study

- X-ray tube: COMET Yxlon EVO200D (200 kV, 6 mA);
- Detection system: Varian PaxScan 2520D flat panel;
- Motion system:
  - CAD Project horizontal and vertical 1.5 m travel range translation axes;
  - CAD Project 1.3 m travel range vertical translation axis for the X-ray source;
  - PI-Micos PRS200 precision rotation stage, 50 kg centred load over an iron adjustable basement.

The system operates mostly in continuous scanning mode with hardware detector binning (pixel size 254 μm), especially for large objects that require a wide scanning grid, to reduce the overall CT time. Typical single-position scanning time is 3 min in this configuration, when it is possible to operate with a detector maximum frame rate of 10 fps. All components, including the translation axes, can be disassembled and loaded separately in a van for transportation, although in this case system reassembly requires significantly more work than for the previous scanner. While the alignment procedure is also more complicated and time consuming, once mounted the system yields excellent performance and is capable of scanning several large-size objects within a single day. While the resolution achievable for large objects is close to 200 μm, in most cases, for 3D rendering purposes of the CT reconstructions, the obtained resolution is around 400 μm. It is possible to scan objects up to 1.2 m in size.

Recent applications of both mobile systems included, in 2023, a few on-site scanning campaigns at the Museo Egizio in Turin, which houses one of the largest holdings of Egyptian antiquities and is considered the second most important collection in the world. Different projects and artefacts required two distinct measurement campaigns, using different instruments and setups, respectively, focusing on small pottery findings from Eliopolis and a number of bigger objects belonging to the tomb of Kha and Merit. On both occasions, the two CT systems operated successfully and the measurement campaigns were completed with satisfying results, confirming the versatile nature and high-performing capabilities of the CHNet Bologna mobile CT systems. An example of the results is shown in Fig. 11.

4.2 X-ray imaging systems at INFN-Turin

Two X-ray imaging systems have been developed within the INFN-CHNet Turin node: one is a CT setup tailored to the analysis of large-scale objects, up to a few metres in dimensions, while the second is a micro-CT setup for small objects. Both systems are currently fixed and cannot be moved away from their location, although an update in terms of portability is being developed for the micro-CT equipment.

4.2.1 Fixed CT system for large-scale objects at CCR "La Venaria Reale"

Located at the Centro per la Conservazione ed il Restauro dei Beni Culturali (CCR) "La Venaria Reale", the setup for large objects was developed between 2009 and 2013 in the framework of the neu_ART project [73], which received funding from the Piedmont Region. Installed in an air-conditioned, shielded environment of about $5 \times 5 \times 3.5$ m^3, the system was specifically designed to enable the DR analysis of paintings up to a few square metres and the CT acquisition of wooden artefacts up to 2.5 m high (Fig. 12a).

The system's main components are described below:

- X-ray source: GE Eresco 42MF4 (200 kV maximum voltage and 3 mm focal spot size);
- Detection system: Hamamatsu C9750-20TCN linear detector (200 μm pixel size);
- Motion system:
  - Newport RV PE 350 rotary stage;
  - two vertical motorised mechanical axes with range of more than 2 m for source and detector;
  - one horizontal axis with a range of 3.5 m and a speed range between 0.2 and 5.0 m/min for the detector.

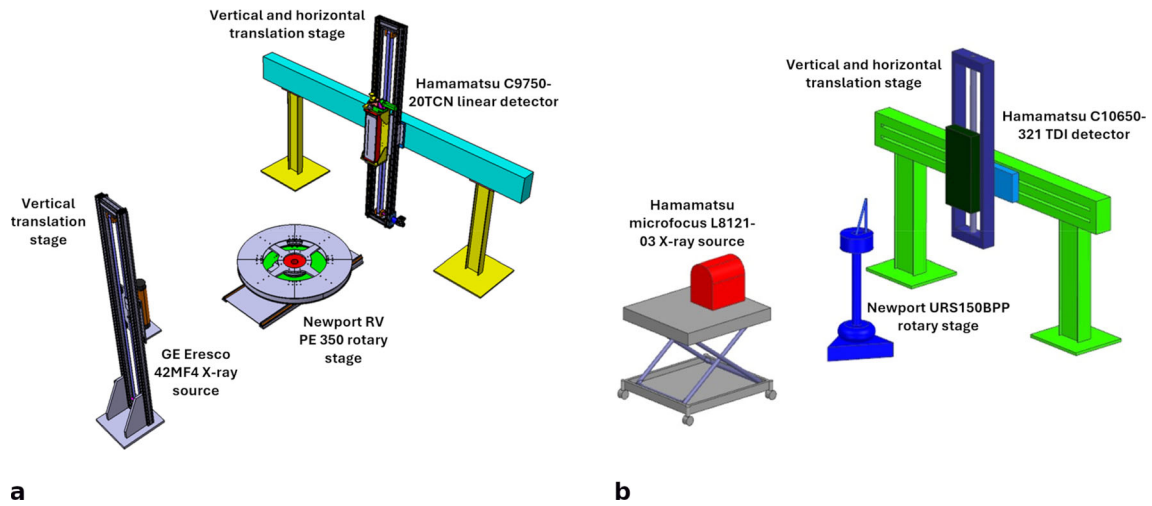

Fig. 12 X-ray imaging systems at the INFN-CHNet Turin node: **a** setup for large objects installed at the CCR "La Venaria Reale" and **b** micro-CT setup for small objects

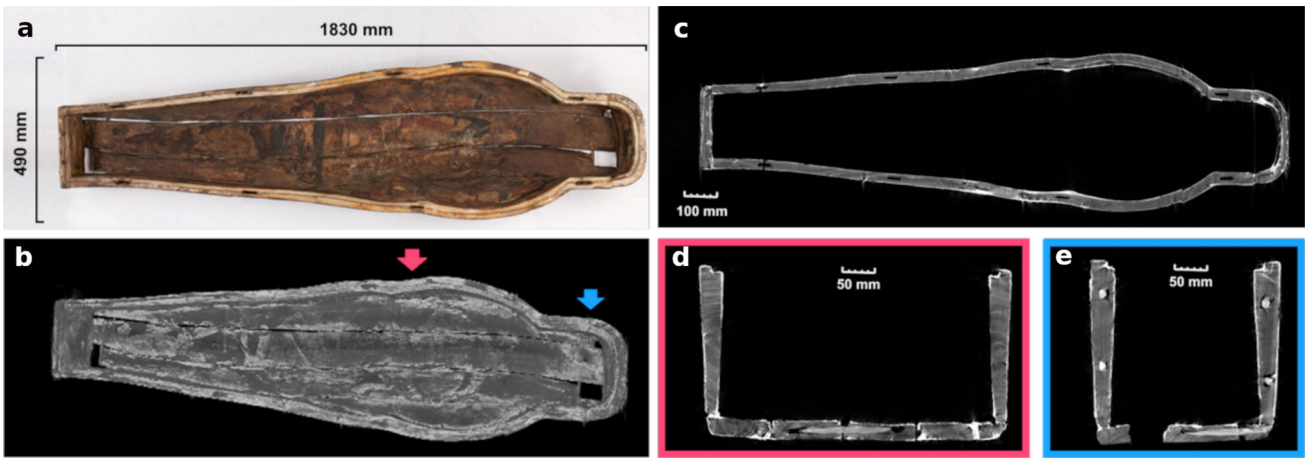

Fig. 13 **a** Visible photograph and **b** CT 3D image of the alveus of Taiefmutmut's coffin (183 cm × 49 cm × 25 cm). **c** Frontal section of the coffin, selected at about half depth. **d**, **e** Transversal sections acquired in correspondence respectively to the blue and red arrow in picture (**b**). CT acquisition parameters are as follows: 180 kV voltage, 5 mA current, 1.2 × magnification, and 0.5 mm voxel size

To limit the signal due to scattered X-rays, the linear detector is placed behind a vertical, 1-cm-thick lead collimator, and its rotation is synchronised with the horizontal translation. The rotary stage is embedded in a structure mounted on a carriage, which enables adjustment of the distance between the object under analysis and the detector according to the size of the object itself.

This setup proved to be very versatile, enabling the radiographic analysis of large paintings [74] and the tomographic investigation of large wooden artefacts, including pieces of furniture [75] and the lid of Taiefmutmut's coffin [76]. Smaller objects made of different materials can also be analysed: for example, a soil block from an archaeological excavation, whose CT revealed a metal belt inside [77]. Recently, the alveus of Taiefmutmut's coffin (Cat. 2228/1 – Museo Egizio, Turin) was investigated: as can be seen in Fig. 13, CT scanning is highly effective in providing insight into the technique used to create the object and its state of preservation. Data collected includes the observation of the growth rings of the wood, useful in assessing the distribution and orientation of the blocks and the joints between them, as well as the detection of any missing pieces, holes, cracks, and any material overlying the wood. In addition, the dimensions and thickness of each element can be evaluated.

Over the last few years, a small flat-panel detector was coupled with different CT setups and other instrumentation (e.g. the MA-XRF in Sect. 2.1.3): it is an 11 cm × 14 cm Teledyne Dalsa Shad-o-Box 6K HS with 49.5 μm pixel (Fig. 12b). The panel can be mounted together with the linear detector on the same mechanical axes, which are used in a fixed configuration and moved only for alignment purposes. This approach is very useful for smaller objects, up to a few tens of cm maximum in each direction, that require scanning at high resolution; good results have already been obtained on small wooden sculptures from the Museo Egizio in Turin, namely two offering bearers [78] and a Taweret goddess showing traces of gilding [79].

4.2.2 *Fixed micro-CT system for small objects in Turin*

A micro-CT setup was developed for acquisitions on smaller objects; the main components of its original configuration include the following:

- X-ray source: Hamamatsu microfocus L8121-03 (150 kV maximum voltage and 5 μm minimum focal spot);
- Detection system: Hamamatsu C10650-321 "linear" TDI detector (220 mm × 6 mm area and 48 μm pixel);
- Motion system:
  - Newport URS150BPP rotary stage;
  - two motorised axes for horizontal and vertical movements of the detector;
  - a vertical axis for manual movement of the source.

The TDI detector can be used in two different ways: mounted vertically in "scan mode", to acquire CT volumes of objects up to a few tens of cm, such as an ancient toy from Cyprus known as tintinnabulum [80]; or mounted horizontally and held fix in "area mode" to collect a few horizontal slices of small objects in a faster way, such as pearls, to determine whether they are of natural or artificial origin based on their inner structures [81].

The flat-panel detector described above can be coupled with the micro-CT system instead of the TDI detector, yielding different advantages: it operates more quickly than the TDI detector in "scan mode" and can capture the entire volume of an object, as opposed to the TDI's "area mode", which is limited to acquiring only a few sections. This approach is also quite versatile: exploiting the magnification, a micro-CT scan of cm-sized objects can be obtained with voxel size below 10 μm, such as beads made of both glass [82] and shell [83]. Increasing the voxel size and using the tile scan, larger objects can be analysed, such as ancient wooden flutes [84].

4.3 X-ray imaging system at INFN-Florence

In the framework of the PNRR PE5 project CHANGES: Cultural Heritage Active Innovation for Sustainable Society, a transportable system for X-ray radiography/tomography is currently being developed. The system is designed for in situ measurements, exploiting a shielding design to accomplish the current radio-safety rules. A low-power X-ray source (50 W) will be installed for this purpose. The shielding will contain the object, the detector, and the translation stages, while the X-ray source will be facing on one side. These characteristics make this equipment suitable for the analysis of small, light objects, such as wooden statuettes, ceramic samples, and bones or shells, and could be employed also in external sites such as museum galleries and storages.

5 Neutron-based imaging

Neutron imaging (NI) techniques generally enable the creation of digital datasets related to the morphology and composition of complex objects. Specifically, radiography entails measuring the intensity of neutrons passing through a sample, which provides information on its density, internal morphology, and the relationship among different elements in a similar way to X-ray radiography. With neutrons, however, it is also possible to analyse significant thicknesses (in the order of centimetres) of heavy materials such as metals. As in the case of X-rays, a neutron tomography of the artefact can be obtained by combining various radiographs at different orientations [85–87]. The possibility to reconstruct an object's entire volume makes every constitutive and microstructural detail virtually explorable [88, 89], proving this tool essential to investigate the manufacturing methodologies and to assess the preservation state [90–92]. In this regard, neutrons offer an invaluable opportunity to map corrosion phenomena across a sample's entire volume in a completely non-invasive way, exploiting the strong interaction that this probe has with hydrogen. As shown in the literature, through its association with other light elements such as oxygen, hydrogen can be used to identify the most mineralised and corroded areas of a metallic artefact [93]. Moreover, for hollow metal objects such as bronze statues, the metal thickness, the presence of fractures, gaps and defects, as well as the presence of inner elements such as support structures or casting cores, can be investigated [94]. Starting from the projection data, it is also possible to reconstruct a 3D model of the entire volume of an object, providing conservators with a highly informative and intuitive tool. Thanks to the different attenuations possibly shown by the artefact components, it is also possible to virtually separate such components by digitally segmenting their distinct volumes.

Neutron imaging techniques, both white beam-NI (WB-NI) and monochromatic-NI (energy selective neutron imaging ES-NI, and Bragg edge neutron transmission analysis, BENT), are currently the probes of choice for a totally non-invasive study of metal artefacts, providing a wealth of information from morphological and microstructural data, to the characterisation of alloys, and to the study of the manufacturing processes used to create cultural heritage objects. Although in Europe several research centres offer the possibility to use beam time for NI experiments, until a few years ago in Italy there was no facility suitable for this purpose.

Table 1 Set-up parameters and performances in NICHE working configurations

Parameter	High flux configuration	High-resolution configuration
Shutter to detector distance	1410 mm	1920 mm
L/D	140	190
FoV (field of view)	Ø 65 mm (*rounded*) 45 mm (*max square side*)	Ø 95 mm (*rounded*) 65 mm (*max square side*)
Spatial resolution		
PSI bar pattern at 40 mm from the scintillator (typical working distance)	180 μm	150 μm
PSI bar pattern sticked to the scintillator (Best spatial resolution)	150 μm	125 μm
Acquisition time		
Optimal	600 s	1200 s
Typical	300 s	600 s
Tomography mode	120 s	240 s

5.1 CHNet-NICHE: the neutron imaging station for cultural heritage in Pavia

In this context, INFN-CHNet spearheaded a project titled *Neutron Imaging in Cultural HEritage* (NICHE), devoted to the development and operation of a neutron imaging station at the 250 kW TRIGA Mark-II reactor managed by the Laboratorio Energia Nucleare Applicata (LENA) in Pavia [89, 95, 96]. The NICHE imaging station is located on the TRIGA thermal beamline port B, which has the best potential for imaging applications as it offers the highest ratio of thermal respect to epithermal + fast neutrons. The epithermal and gamma flux are furthermore lowered by 70-mm bismuth and 100-mm sapphire filters contained in the flight tube, making the neutron flux in the sample area on the order of 2×10^5 cm^{-2} s^{-1}.

The main instrumental components are the following:

- experimental hutch, main area size: 2.5 m length, 0.6 m width, 2.1 m height, entrance area with maze double corner;
- remotely controlled beam shutter;—pin-hole selector made of interchangeable ceramic cartridges of 8 mm thick (10 or 20 mm diameter aperture);
- manipulation: x–z–ω motorised movement (typical working sample-to-detector distance: 40 mm);
- acquisition system: Cu doped 300 μm thickness LiF/ZnS scintillator screen coupled with CMOS digital camera (16 bit), 20 mm optic lens on a remotely controlled translation stage for focusing; camera pixel size corresponds on the scintillator to 50 μm × 50 μm area;
- LabVIEW-based remote control interface allowing to perform script sequence of commands (motor movement and acquisition).

Despite the limited dimensions of the experimental hutch, exploiting a rail system that allows the independent movement of the camera box and sample holder, NICHE offers two working configurations (Table 1), with different *L*/*D* (collimation ratio) values, where *L* represents the distance from the aperture to the image plane, and *D* is the diameter of the aperture. A lower *L*/*D* value results in more pronounced blurring in the image compared to the inherent unsharpness caused by the imaging device. As the *L*/*D* ratio increases, the level of unsharpness decreases, leading to an improvement in image quality. Due solely to geometric factors, the neutron beam profile tends to become flatter at the image plane as the *L*/*D* ratio increases.

The station was established in April 2021, working for the equivalent of 30 beam time days to date. The components are easy to remove and install and the complete setup takes about 2 h.

Numerous test experiments on different materials were performed including some objects that could be representative of archaeological samples. Figures 14 and 15 show two representative examples. Figure 14 illustrates the neutron radiograph of a fifth century B.C. bronze decorative artefact from the Balkan area. The artefact's thickness is nearly constant; this allows one to obtain relevant information even with a simple radiogram, in which the contributions of the attenuations along the sample thickness are not resolved, but are instead represented by an average of the attenuations of the various phases stacked in a two-dimensional image.

Despite this, some variations in the grey values can be noticed, which can be attributed to morphological differences (Fig. 14b). Furthermore, it is possible to propose a mapping of the areas most affected by corrosion based on the H detection (dark grey-black areas, Fig. 14c/orange–red–purple areas in the false coloured image).

The second example shows the result of the reconstructed data of a white beam—neutron tomography (WB-NT) experiment on a 19th-century Japanese copper alloy sword fitting (Fuchi) (Fig. 15). Figure 15b displays different slices orientation, exploiting, aside from the orthogonal reorientation, a radial reslice that allows one to visualise, on a single plane, parts of the object that are lying on different planes. This method [97] is used here to investigate the side of the Fuchi just a few micrometres below the object's

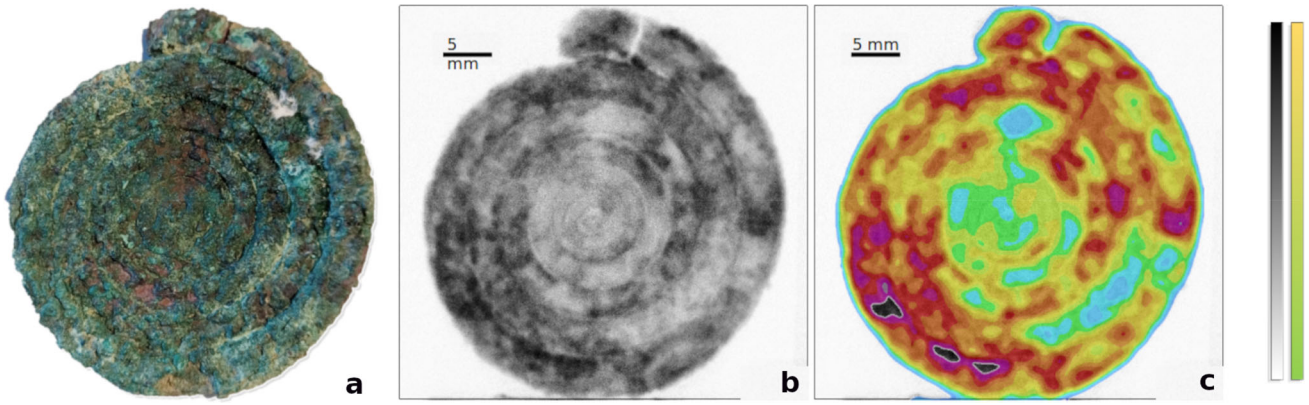

Fig. 14 **a** Ancient bronze spiral from South-East Europe, Balkan area, fifth century B.C.E. (private collection). **b** Normalised white beam neutron radiography: high corroded areas appear darker due to a greater attenuation power of the mineralised phases that are rich in H. **c** False colour map of the attenuation power, enabling the mapping of corrosion for this archaeological sample

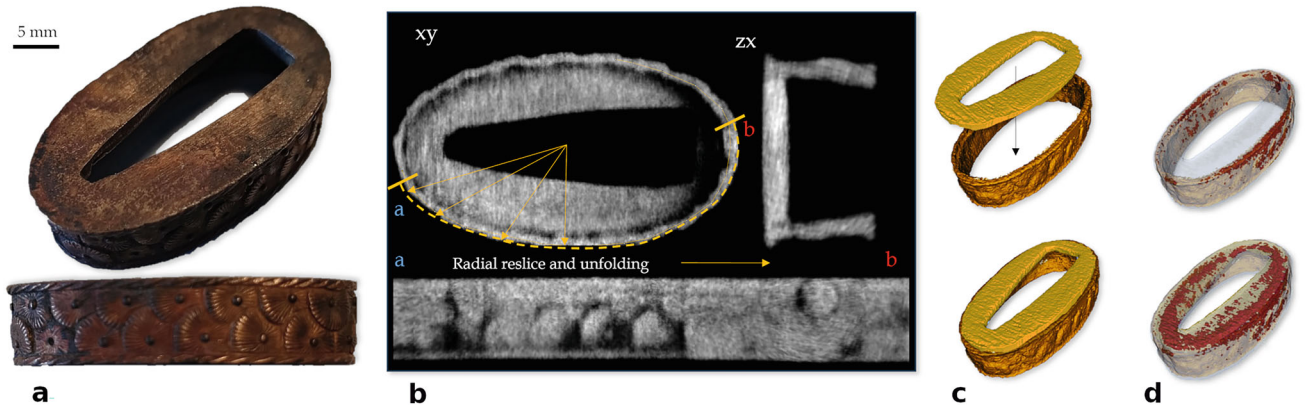

Fig. 15 White Beam Neutron Tomography (WB-NT) of a copper alloy nineteenth century Japanese sword fitting (Fuchi): **a** picture of the object; **b** on the top are shown axial (*xy*) and normal (*zx*) slices; on the bottom it is shown, in a single plane, the side decoration of the Fuchi, obtained exploiting a radial reslice and unfolding process (as described in [97]). WB-NT 3D segmentation allows us to visualise the two different parts that constitute the Fuchi (**c**), while in (**d**) the 3D corrosion map is shown

surface. In Fig. 15c and d, the artefact's manufacturing technique (c) and the 3D corrosion map (d) were obtained by means of 3D segmentation.

6 Conclusions and future perspectives

INFN created its Cultural Heritage Network, INFN-CHNet, to promote the development and application of scientific methods and technologies to cultural heritage materials and artefacts. In this framework, a series of instruments with different technical features and prospective applications have been developed by INFN researchers over the years. Among these, the wide array of X-ray and neutron-based imaging techniques available within INFN-CHNet was showcased in this paper.

Concerning X-ray imaging, several MA-XRF systems are currently available within the network, allowing for in situ elemental mapping of relatively large surfaces (up to 300×300 mm^2) in a great variety of samples and objects, with a spatial resolution in the hundreds of micrometres range. MA-XRF is a powerful technique mainly used for the elemental characterisation of pigments in paintings and other bidimensional surfaces, but also successfully employed to identify inorganic materials in a large variety of objects, such as furniture, pottery, mosaics, or metal artefacts.

Some of the instruments discussed above are based on the coupling of XRF with complementary techniques for a more comprehensive characterisation of the object's materials:

XRL for the study of minerals and gemstones, whose luminescence properties can provide useful information for an exhaustive materials characterisation. A provenance study on lapis lazuli artefacts was reported in this article as an example.

DR for the visualisation of a sample's inner features. In the study of paintings, this technique might shed light on the structural elements, preparation layer, and paint materials. In some cases, it may highlight the presence of hidden features and compositional changes, such as pentimenti. In tridimensional objects like pottery and wooden artefacts, DR often yields valuable information on

the fabrication techniques. In addition, radiography can be helpful in assessing an object's preservation state and in the identification of forgeries.

Reflection FTIR for the molecular characterisation of a sample's organic and inorganic components, enabling the identification of pigments, fillers, binders, and degradation products in various paint materials. This technique is also used to identify textile fibres and, more broadly, to shed light on the chemical composition, deterioration processes, and conservation products across a wide range of materials, including paper, polymers, stone, ceramic, and glass.

UV-induced fluorescence spectroscopy (or photoluminescence) allows the characterisation of both organic and inorganic materials such as binders, dyes, pigments, and degradation products. This technique enables the discrimination of materials through their characteristic emission spectra and decay times. It is useful to define the conservation state of the analysed artworks and to discriminate among original and restored areas.

Laser profilometry to measure the sample's surface roughness with micrometric resolution. This method allows for the identification of concealed details, such as traces of the tools used by artists in the preliminary phases of a composition, providing valuable insights into the techniques employed. By conducting repeated surveys at various times one can detect changes in the object shape and variations in surface layer thickness, particularly during cleaning processes.

PIXE imaging is available at MACHINA, the newly developed transportable particle accelerator for cultural heritage applications; here, the elemental imaging system is based on sample scanning under a fixed beam, with a spatial resolution in the range of some hundreds of micrometres and a maximum scanned area currently corresponding to 600×200 mm^2. Similarly to XRF, PIXE is employed for the elemental characterisation of inorganic materials found in paintings and a wide range of different objects, including furniture, pottery, mosaics, and metals. This technique enables quantitative measurements, even down to trace elements, and has the capability to offer insight into the composition at varying depths by adjusting the proton energy and, consequently, the probed depth.

In addition, X-ray DR and CT systems are also available for objects of different size, such as paintings up to a few square metres and wooden artefacts up to 2.5 m high, and with different resolution, down to 4.5 μm voxel dimension for small objects. Some of the instrumentation discussed in this article is portable, allowing for in situ analysis of the artefacts. DR and CT enable us to reconstruct the inner structure of an artefact, thus shedding light on its construction techniques, preservation state, and materials composition. They can be applied to nearly all types of artefacts, provided that the dimensions are appropriate for setup within the system used. However, when using standard instrumentation, these techniques are scarcely informative in case of large high Z-high density artefacts, such as large metal or stone sculptures, which typically completely absorb the X-rays produced by standard tubes and would require higher energy sources, such as linac [98]. Furthermore, organic materials, especially when embedded in higher density objects, are hardly evidenced.

All these limitations can be overcome by using the same techniques with neutron beams as probes. As in X-ray tomography, in neutron tomography the entire volume of an object can be reconstructed, allowing for the virtual exploration of every constitutive detail and thus offering a fundamental tool to investigate the manufacturing methods and assess the preservation state. Differently from X-rays, neutrons allow one to analyse heavy materials such as metals with significant thicknesses (in the order of centimetres), with the added ability to detect the inner presence of organic materials. Thanks to the high sensitivity to hydrogen, neutrons enable to map the corrosion on a sample's entire volume in a completely non-invasive manner, thus contributing to the assessment of an artefact's preservation state.

At INFN-CHNet, a neutron imaging station at the TRIGA Mark-II reactor of LENA in Pavia was developed within the NICHE project. Tailored to the analysis of objects with mass within 5 kg, not highly radiopaque, and with dimensions up to about ten cm in width and depth and about twenty in height (or more considering stitching procedure), with 125 μm resolution (best possible configuration), NICHE is the first Italian neutron imaging station dedicated to cultural heritage. Despite the low flux and the limited availability of beam time due to the radioprotection limits at LENA, NICHE has a great potential as a tool for the analysis of CH artefacts via radiographs and neutron tomography.

All the above-discussed techniques provide an output in the form of images, which always require post-processing to interpret the results correctly and to extract legible data to be shared with art historians, conservators, and other stakeholders. In the field of image treatment, significant efforts are currently being focused on the application of statistical methods and deep learning to imaging raw data. By identifying patterns and correlations in the data, these algorithms offer valuable insights into the composition, age, and condition of the artefact [99–108] (for other Machine learning approaches in Cultural Heritage, see [109], and references therein).

Acknowledgements INFN-LNF authors would like to thank LAZIO INNOVA for the financial support of ARTEMISIA project: Det. G07413 del 16.06.2021, pubblicata sul BURL n. 61 del 22.06.2021, Atto di Impegno del 18.10.2021, Avviso pubblico di LAZIO INNOVA, società in house della Regione Lazio, Accordo di programma quadro "Ricerca, Innovazione Tecnologica, Reti Telematiche" (APQ6) - Stralcio "Attuazione degli interventi programmatici e dei nuovi interventi relativi al Distretto Tecnologico per le nuove tecnologie applicate ai beni e alle attività culturali". Intervento TE1 - Invito al Centro di Eccellenza a presentare progetti per la seconda fase - Progetti RSI. INFN-Roma Tre and Roma Tre University authors would like to thank Fondazione Roma (Grant No. 5229441F37) and Regione Lazio under the Project PERSEPOLY - CUP I85F21000930002 for research funding. The authors also acknowledge funding from the European Union - NextGenerationEU- CHANGES – CUP B83C22005060006 Project code: PE00000020, "Istruzione e ricerca" - Componente 2 "Dalla ricerca all'impresa" - Investimento 1.3, Partenariato Esteso 5 through the Excellence Centre at the Lazio Technological District for Cultural Heritage (DTC Lazio) and Spoke 5 "Science and technologies for sustainable diagnostics for cultural heritage" - WP1 "Advanced non-invasive methods for sustainable

diagnostics in Heritage Science" (UniFi). Finally, the authors would like to thank the Direction of the Gallerie Nazionali, the chief of the Restoration Laboratory Chiara Merucci and art curator Alessandro Cosma for authorising and making possible the measurements of the artwork L'ebbrezza di Noè.

Funding Open access funding provided by Università degli Studi di Firenze within the CRUI-CARE Agreement.

Data Availability Statement The manuscript has associated data in a data repository. [Authors' comment: Data sets reported in the current study are available from the corresponding authors on reasonable request.]

References

1. G. Bitossi, R. Giorgi, M. Mauro, B. Salvadori, L. Dei, Spectroscopic techniques in cultural heritage conservation: a survey. Appl. Spectrosc. Rev. **40**, 187–228 (2005). https://doi.org/10.1081/ASR-200054370
2. I. Liritzis, E. Korka, Archaeometry's role in cultural heritage sustainability and development. Sustainability **11**, 1972 (2019). https://doi.org/10.3390/su11071972
3. M. Alfeld, L. de Viguerie, Recent developments in spectroscopic imaging techniques for historical paintings—a review. Spectrochim. Acta Part B **136**, 81–105 (2017). https://doi.org/10.1016/j.sab.2017.08.003
4. B.H. Berrie, Rethinking the history of artists' pigments through chemical analysis. Annu. Rev. Anal. Chem. **5**, 441–459 (2012). https://doi.org/10.1146/annurev-anchem-062011-143039
5. D. Bersani, C. Conti, P. Matousek, F. Pozzi, P. Vandenabeele, Methodological evolutions of Raman spectroscopy in art and archaeology. Anal. Methods **8**, 8395–8409 (2016). https://doi.org/10.1039/C6AY02327D
6. T. Calligaro, A. Banas, K. Banas, I. Radovic, M. Brajkovic, M. Chiari, A. Forss, I. Hajdas, M. Krmpotic, A. Mazzinghi et al., Emerging nuclear methods for historical painting authentication: AMS-C-14 dating, MeV-SIMS and O-PTIR imaging, global IBA, differential-PIXE and full-field PIXE mapping. Forensic Sci. Int. (2022). https://doi.org/10.1016/j.forsciint.2022.111327
7. P. Ricciardi, K.A. Dooley, D. MacLennan, G. Bertolotti, F. Gabrieli, C.S. Patterson, J.K. Delaney, Use of standard analytical tools to detect small amounts of smalt in the presence of ultramarine as observed in 15th-century Venetian illuminated manuscripts. Herit. Sci. **10**, 38 (2022). https://doi.org/10.1186/s40494-022-00671-z
8. V. Ciaramitaro, F. Armetta, M. Saladino, M.L. Saladino, The colours of Segesta. Searching for the traces of the lost pigments. J. Cult. Herit. **59**, 30–37 (2023). https://doi.org/10.1016/j.culher.2022.11.003
9. L. Sottili, L. Giuntini, A. Mazzinghi, M. Massi, L. Carraresi, L. Castelli, C. Czelusniak, F. Giambi, P. Mando, M. Manetti et al., The role of PIXE and XRF in heritage science: the INFN-CHNet LABEC experience. Appl. Sci. Basel (2022). https://doi.org/10.3390/app12136585
10. P. Weibring, T. Johansson, H. Edner, S. Svanberg, B. Sundnr, V. Raimondi, G. Cecchi, L. Pantani, Fluorescence lidar imaging of historical monuments. Appl. Opt. **40**, 6111–6120 (2001). https://doi.org/10.1364/AO.40.006111
11. INFN CHNet. https://chnet.infn.it/en/about/. Accessed 05 June 2023
12. L. Giuntini, L. Castelli, M. Massi, M. Fedi, C. Czelusniak, N. Gelli, L. Liccioli, F. Giambi, C. Ruberto, A. Mazzinghi et al., Detectors and cultural heritage: the INFN-CHNet experience. Appl. Sci. Basel (2021). https://doi.org/10.3390/app11083462
13. M.J. Nuevo, A. Martín Sánchez, Application of XRF spectrometry to the study of pigments in glazed ceramic pots. Appl. Radiat. Isot. **69**, 574–579 (2011). https://doi.org/10.1016/j.apradiso.2010.11.025
14. L. Castelli, L. Giuntini, F. Taccetti, E. Barzagli, F. Civita, C. Czelusniak, M. Fedi, N. Gelli, F. Grazzi, A. Mazzinghi et al., New criterion for in situ, quick discrimination between traditionally maintained and artificially restored Japanese swords (katanas) by XRF spectroscopy. X-Ray Spectrom. **42**, 537–540 (2013). https://doi.org/10.1002/xrs.2516
15. F.A.C.R.A. Sanches, R.C. Nardes, R.S. Santos, H.S. Gama Filho, A.S. Machado, R.G. Leitão, C.C.G. Leitão, T.E. Calgam, R. Bueno, J.T. Assis et al., Characterization an wooden Pietà sculpture from the XVIII century using XRF and microct techniques. Radiat. Phys. Chem. **202**, 110556 (2023). https://doi.org/10.1016/j.radphyschem.2022.110556
16. R. Cesareo, A. Brunetti, S. Ridolfi, Pigment layers and precious metal sheets by energy-dispersive x-ray fluorescence analysis. X-Ray Spectrom. **37**, 309–316 (2008). https://doi.org/10.1002/xrs.1078
17. A. Mazzinghi, L. Giuntini, N. Gelli, C. Ruberto, XRF study on the gilding technique of the fresco "Crocifissione con Santi" by Beato Angelico in the San Marco monastery in Florence. X-Ray Spectrom. **45**, 28–33 (2016). https://doi.org/10.1002/xrs.2650
18. S. Saverwyns, C. Currie, E. Lamas-Delgado, Macro X-ray fluorescence scanning (MA-XRF) as tool in the authentication of paintings. Microchem. J. **137**, 139–147 (2018). https://doi.org/10.1016/j.microc.2017.10.008
19. G. Van der Snickt, S. Legrand, I. Slama, E. Van Zuien, G. Gruber, K. Van der Stighelen, L. Klaassen, E. Oberthaler, K. Janssens, In situ macro X-ray fluorescence (MA-XRF) scanning as a non-invasive tool to probe for subsurface modifications in paintings by PP Rubens. Microchem. J. **138**, 238–245 (2018). https://doi.org/10.1016/j.microc.2018.01.019
20. H.C. Santos, C. Caliri, L. Pappalardo, F. Rizzo, F.P. Romano, MA-XRF and XRD analysis revealing a polychrome Centuripe vase. J. Archaeol. Sci. Rep. **35**, 102760 (2021). https://doi.org/10.1016/j.jasrep.2020.102760
21. E. Kokiasmenou, C. Caliri, V. Kantarelou, A.G. Karydas, F.P. Romano, H. Brecoulaki, Macroscopic XRF imaging in unravelling polychromy on Mycenaean wall-paintings from the Palace of Nestor at Pylos. J. Archaeol. Sci. Rep. **29**, 102079 (2020). https://doi.org/10.1016/j.jasrep.2019.102079
22. S. Legrand, G. Van der Snickt, S. Cagno, J. Caen, K. Janssens, MA-XRF imaging as a tool to characterize the 16th century heraldic stained-glass panels in Ghent Saint Bavo Cathedral. J. Cult. Herit. **40**, 163–168 (2019). https://doi.org/10.1016/j.culher.2019.06.003
23. A. Mazzinghi, C. Ruberto, L. Giuntini, P. Mando, F. Taccetti, L. Castelli, Mapping with macro X-ray fluorescence scanning of Raffaello's Portrait of Leo X. Heritage **5**, 3993–4005 (2022). https://doi.org/10.3390/heritage5040205
24. M. Alfeld, J.V. Pedroso, M. van Eikema Hommes, G. Van der Snickt, G. Tauber, J. Blaas, M. Haschke, K. Erler, J. Dik, K. Janssens, A mobile instrument for in situ scanning macro-XRF investigation of historical paintings. J. Anal. At. Spectrom. **28**, 760–767 (2013). https://doi.org/10.1039/C3JA30341A

25. F.P. Romano, C. Caliri, P. Nicotra, S. Di Martino, L. Pappalardo, F. Rizzo, H.C. Santos, Real-time elemental imaging of large dimension paintings with a novel mobile macro X-ray fluorescence (MA-XRF) scanning technique. J. Anal. At. Spectrom. **32**, 773–781 (2017). https://doi.org/10.1039/C6JA00439C
26. ELIO. https://www.bruker.com/en/products-and-solutions/elemental-analyzers/micro-xrf-spectrometers/elio.html. Accessed 14 Feb 2024
27. F. Taccetti, L. Castelli, C. Czelusniak, N. Gelli, A. Mazzinghi, L. Palla, C. Ruberto, C. Censori, A. Lo Giudice, A. Re et al., A multipurpose X-ray fluorescence scanner developed for in situ analysis. Rendiconti Lincei-Scienze Fisiche e Naturali **30**, 307–322 (2019). https://doi.org/10.1007/s12210-018-0756-x
28. C. Ruberto, The mission of the INFN-Cultural Heritage Network: the multifaceted example of the Macro-XRF scanner experience. Rendiconti Lincei. Scienze Fisiche e Naturali **34**, 889–906 (2023). https://doi.org/10.1007/s12210-023-01175-z
29. QT. https://www.qt.io/developers/. Accessed 13 Feb 2024
30. A. Mazzinghi, C. Ruberto, L. Castelli, P. Ricciardi, C. Czelusniak, L. Giuntini, P. Mando, M. Manetti, L. Palla, F. Taccetti, The importance of being little: MA-XRFon manuscripts on a Venetian island. X-Ray Spectrom. **50**, 272–278 (2021). https://doi.org/10.1002/xrs.3181
31. L. Sottili, L. Guidorzi, A. Mazzinghi, C. Ruberto, L. Castelli, C. Czelusniak, L. Giuntini, M. Massi, F. Taccetti, M. Nervo et al., The importance of being versatile: INFN-CHNet MA-XRF scanner on furniture at the CCR "La Venaria Reale." Appl. Sci. Basel (2021). https://doi.org/10.3390/app11031197
32. A. Mazzinghi, L. Castelli, F. Giambi, C. Ruberto, L. Sottili, F. Taccetti, L. Giuntini, The importance of preventive analysis in heritage science: MA-XRF supporting the restoration of Madonna with child by Mantegna. Appl. Sci. **13**, 7983 (2023). https://doi.org/10.3390/app13137983
33. F. Taccetti, L. Castelli, C. Czelusniak, F. Giambi, M. Manetti, M. Massi, A. Mazzinghi, C. Ruberto, F. Arneodo, R. Torres et al., Novel implementation of the INFN-CHNet X-ray fluorescence scanner for the study of ancient photographs, archaeological pottery, and rock art. Rendiconti Lincei. Scienze Fisiche e Naturali **34**, 515–522 (2023). https://doi.org/10.1007/s12210-023-01143-7
34. G. Bartolozzi, A. Casini, L. Castelli, C. Cucci, F. Grazzi, A. Mazzinghi, I. Pieralli, C. Ruberto, R. Sarfati, A. Sidoti et al., The non-invasive spectroscopic study of a parchment object from the national central library of florence: the Hebrew scroll. Heritage **7**, 206–224 (2024). https://doi.org/10.3390/heritage7010011
35. MOXTEK MAGPRO. https://moxtek.com//wp-content/uploads/pdfs/TUB-DATA-1013-MAGPRO.pdf. Accessed 14 Feb 2024
36. Ocean Optics. https://www.oceaninsight.com/products/spectrometers/high-sensitivity/qepro-series/. Accessed 14 Feb 2024
37. Dalsa Teledyne. https://www.teledynedalsa.com/en/products/imaging/industrial-x-ray/shad-o-box-hs/. Accessed 09 Feb 2024
38. Sottili, L., Design and development of a benchtop X-ray based instrument and its heritage science applications. Doctoral thesis, University of Turin (2023)
39. L. Sottili, L. Guidorzi, A. Lo Giudice, A. Mazzinghi, C. Ruberto, L. Castelli, C. Czelusniak, L. Giuntini, M. Massi, F. Taccetti et al., Macro X-ray fluorescence analysis of XVI-XVII century Italian paintings and preliminary test for developing a combined fluorescence apparatus with digital radiography. ACTA IMEKO (2022). https://doi.org/10.21014/acta_imeko.v11i1.1088
40. N. Sanna, Le sculture lignee del gabinetto di Palazzo Granieri: studio, conservazione e approfondimenti su tecniche di imitazione "alla China" e patinature ottocentesche (2020)
41. L. Guidorzi, A. Re, M. Magalini, D. Angelici, A. Borghi, G. Vaggelli, F. Fantino, V. Rigato, L. La Torre, Q. Lemasson et al., Micro-PIXE and micro-IBIL characterization of lapis lazuli samples from Myanmar mines and implications for provenance study. Eur. Phys. J. Plus **138**, 175 (2023). https://doi.org/10.1140/epjp/s13360-023-03768-x
42. A. Lo Giudice, A. Re, S. Calusi, L. Giuntini, M. Massi, P. Olivero, G. Pratesi, M. Albonico, E. Conz, Multitechnique characterization of lapis lazuli for provenance study. Anal. Bioanal. Chem. **395**, 2211–2217 (2009). https://doi.org/10.1007/s00216-009-3039-7
43. A. Re, M. Zangirolami, D. Angelici, A. Borghi, E. Costa, R. Giustetto, L. Gallo, L. Castelli, A. Mazzinghi, C. Ruberto et al., Towards a portable X-ray luminescence instrument for applications in the Cultural Heritage field. Eur. Phys. J. Plus (2018). https://doi.org/10.1140/epjp/i2018-12222-8
44. R. Moreau, T. Calligaro, L. Pichon, B. Moignard, S. Hermon, I. Reiche, A multimodal scanner coupling XRF, UV–Vis–NIR photoluminescence and Vis–NIR–SWIR reflectance imaging spectroscopy for cultural heritage studies. X-Ray Spectrom. (2023). https://doi.org/10.1002/xrs.3364
45. F. Gabrieli, K.A. Dooley, M. Facini, J.K. Delaney, Near-UV to mid-IR reflectance imaging spectroscopy of paintings on the macroscale. Sci. Adv. **5**, eaaw7794 (2019). https://doi.org/10.1126/sciadv.aaw7794
46. G. Capobianco, L. Pronti, E. Gorga, M. Romani, M. Cestelli-Guidi, S. Serranti, G. Bonifazi, Methodological approach for the automatic discrimination of pictorial materials using fused hyperspectral imaging data from the visible to mid-infrared range coupled with machine learning methods. Spectrochim. Acta Part A Mol. Biomol. Spectrosc. **304**, 123412 (2024). https://doi.org/10.1016/j.saa.2023.123412
47. P. Almeida, C. Montagner, R. Jesus, N. Correia, M. Vilarigues, M.J. Melo, S. Nascimento, Analysis of paintings using multi-sensor data, in *Proceedings of the 21st European Signal Processing Conference (EUSIPCO 2013)* (2013)
48. A. Cosma, M. Merucci, S. Ridolfi, Raffaello da vicinoNuove indagini e nuove scoperte sulla *Fornarina*. *Saggi in Officina* (2023)
49. S.A. Barcellos Lins, S. Ridolfi, G.E. Gigante, R. Cesareo, M. Albini, C. Riccucci, G. di Carlo, A. Fabbri, P. Branchini, L. Tortora, Differential X-ray attenuation in MA-XRF analysis for a non-invasive determination of gilding thickness. Front. Chem. (2020). https://doi.org/10.3389/fchem.2020.00175
50. S.A. Barcellos Lins, M. Manso, G.E. Gigante, R. Cesareo, L. Tortora, P. Branchini, S. Ridolfi, Modular MA-XRF scanner potentialities and further advances, in *Proceedings of the 2020 IMEKO TC-4 International Conference on Metrology for Archaeology and Cultural Heritage, Trento, Italy* (2020)
51. S.A. Barcellos Lins, M. Manso, P.A.B. Lins, A. Brunetti, A. Sodo, G.E. Gigante, A. Fabbri, P. Branchini, L. Tortora, S. Ridolfi, Modular MA-XRF scanner development in the multi-analytical characterisation of a 17th century Azulejo from Portugal. Sensors **21**, 1913 (2021). https://doi.org/10.3390/s21051913
52. R. Bellucci, P. Carcagni, A. Della Patrib, R. Fontanc, C. Frosinini, M.C. Gambino, M. Greco, M. Mastroianni, M. Materazzi, E. Pampaloni et al., Integration of image data from 2D and 3D optical techniques for painting conservation applications. Imaging Sci. J. **55**, 80–89 (2007). https://doi.org/10.1179/174313107X145209
53. C. Daffara, S. Mazzocato, G. Marchioro, Optical surface metrology for heritage science: proof of concept and critical-constructive discussion, in *Proceedings of the Proceedings of SPIE—The International Society for Optical Engineering* (2023)
54. T. Hanes, P. Hvizdoš, M. Ťavodová, D. Kalincová, J. Hricová, P. Beňo, Coating surface roughness measurement made on coining dies. Manuf. Technol. J. **14**, 309–317 (2014). https://doi.org/10.21062/ujep/x.2014/a/1213-2489/MT/14/3/309
55. C. Colombo, C. Daffara, R. Fontana, M.C. Gambino, M. Mastroianni, E. Pampaloni, M. Realini, A. Sansonetti, Evaluation by laser micro-profilometry of morphological changes induced on stone materials by laser cleaning, in *Proceedings of the Lasers in the Conservation of Artworks* (2007), pp. 523–526
56. R. Fontana, A. Dal Fovo, J. Striova, L. Pezzati, E. Pampaloni, M. Raffaelli, M. Barucci, Application of non-invasive optical monitoring methodologies to follow and record painting cleaning processes. Appl. Phys. A **121**, 957–966 (2015). https://doi.org/10.1007/s00339-015-9505-5
57. keyence. https://www.keyence.it. Accessed 30 May 2024
58. intelligent actuator. https://www.intelligentactuator.com/partsearch2/RCP6(S)-SA6C_p15-16.pdf. Accessed 14 Feb 2024
59. Scissor elevating platform. https://docs.rs-online.com/b7b2/0900766b81718c6a.pdf. Accessed 14 Feb 2024

60. V. Graziani, G. Iorio, P. Branchini, L. Tortora, Fast monitoring of corroding objects by optical profilometry, in *Proceedings of the XIV International Conference AIES, Naples, Italy, 14–15 December 2023* (2023)
61. V. Graziani, G. Iorio, S. Ridolfi, C. Merucci, P. Branchini, L. Tortora, Pigments and brush strokes: investigating the painting techniques using MA-XRF and laser profilometry, in *Proceedings of the Image Analysis and Processing—ICIAP 2023 Workshops, Cham, 2024* (2024), pp. 215–226
62. M. Chiari, External beam IBA measurements for cultural heritage. Appl. Sci. **13**, 3366 (2023). https://doi.org/10.3390/app13053366
63. L. Bertrand, S. Schöeder, D. Anglos, M.B.H. Breese, K. Janssens, M. Moini, A. Simon, Mitigation strategies for radiation damage in the analysis of ancient materials. TrAC Trends Anal. Chem. **66**, 128–145 (2015). https://doi.org/10.1016/j.trac.2014.10.005
64. F. Taccetti, L. Castelli, M. Chiari, C. Czelusniak, S. Falciano, M. Fedi, F. Giambi, P.A. Mandò, M. Manetti, M. Massi et al., MACHINA, the movable accelerator for cultural heritage in-situ non-destructive analysis: project overview. Rendiconti Lincei. Scienze Fisiche e Naturali **34**, 427–445 (2023). https://doi.org/10.1007/s12210-022-01120-6
65. F. Casali, X-ray and neutron digital radiography and computed tomography for cultural heritage, in *Physical Techniques in the Study of Art, Archaeology and Cultural Heritage*. ed. by D. Bradley, D. Creagh (Elsevier, Amsterdam, 2006), pp.41–123
66. M. Rossi, F. Casali, S.V. Golovkin, V.N. Govorun, Digital radiography using an EBCCD-based imaging device. Appl. Radiat. Isot. **53**, 699–709 (2000). https://doi.org/10.1016/S0969-8043(00)00208-6
67. M. Bettuzzi, R. Brancaccio, F. Casali, S. Cornacchia, M. Giordano, M.P. Morigi, A. Pasini, D. Romani, Innovative systems for digital radiography and computed tomography: applications for cultural heritage diagnostics, in *Physics Methods in Archaeometry*. ed. by M. Martini, M. Milazzo, M. Piacentini (IOS Press, Amsterdam, 2004)
68. M. Rossi, F. Casali, P. Chirco, M. Morigi, E. Nava, E. Querzola, M. Zanarini, X-ray 3D computed tomography of bronze archaeological samples. IEEE Trans. Nucl. Sci. **46**, 897–903 (1999). https://doi.org/10.1109/23.790700
69. G. Schena, S. Favretto, L. Santoro, A. Pasini, M. Bettuzzi, F. Casali, L. Mancini, Detecting microdiamonds in kimberlite drill-hole cores by computed tomography. Int. J. Miner. Process. **75**, 173–188 (2005). https://doi.org/10.1016/j.minpro.2004.07.034
70. M.P. Morigi, F. Casali, M. Bettuzzi, D. Bianconi, R. Brancaccio, S. Cornacchia, A. Pasini, A. Rossi, A. Aldrovandi, D. Cauzzi, CT investigation of two paintings on wood tables by Gentile da Fabriano. Nucl. Instrum. Methods Phys. Res. Sect. A **580**, 735–738 (2007). https://doi.org/10.1016/j.nima.2007.05.140
71. M.P. Morigi, F. Casali, A. Berdondini, M. Bettuzzi, D. Bianconi, R. Brancaccio, A. Castellani, V. D'Errico, A. Pasini, A Rossi, X-ray 3D computed tomography of large objects: investigation of an ancient globe created by Vincenzo Coronelli, in *Proceedings of the O3A: Optics for Arts, Architecture, and Archaeology* (2007), pp. 77–84
72. F. Albertin, L.E. Baumer, M. Bettuzzi, R. Brancaccio, E. Caruso, F. Casali, L. Cifarelli, G. Festa, M.G. Griffo, A. Mistretta et al., X-ray computed tomography to study archaeological clay and wood artefacts at Lilybaeum. Eur. Phys. J. Plus **136**, 513 (2021). https://doi.org/10.1140/epjp/s13360-021-01465-1
73. A. Re, F. Albertin, C. Bortolin, R. Brancaccio, P. Buscaglia, J. Corsi, G. Cotto, G. Dughera, E. Durisi, W. Ferrarese et al., Results of the Italian neu_ART project. IOP Conf. Ser. Mater. Sci. Eng. **37**, 012007 (2012). https://doi.org/10.1088/1757-899X/37/1/012007
74. A. Lo Giudice, J. Corsi, G. Cotto, G. Mila, A. Re, C. Ricci, R. Sacchi, L. Visca, L. Zamprotta, N. Pastrone, et al., A new digital radiography system for paintings on canvas and on wooden panels of large dimensions, in *2017 IEEE International Instrumentation and Measurement Technology Conference (I2MTC)* (2017), pp. 1–6
75. A. Re, F. Albertin, C. Avataneo, R. Brancaccio, J. Corsi, G. Cotto, S. De Blasi, G. Dughera, E. Durisi, W. Ferrarese et al., X-ray tomography of large wooden artworks: the case study of "Doppio corpo" by Pietro Piffetti. Herit. Sci. **2**, 19 (2014). https://doi.org/10.1186/s40494-014-0019-9
76. A. Re, A. Lo Giudice, M. Nervo, P. Buscaglia, P. Luciani, M. Borla, C. Greco, The importance of tomography studying wooden artefacts: a comparison with radiography in the case of a coffin lid from ancient Egypt. Int. J. Conserv. Sci. **7**, 935–944 (2016)
77. A. Re, J. Corsi, M. Demmelbauer, M. Martini, G. Mila, C. Ricci, X-ray tomography of a soil block: a useful tool for the restoration of archaeological finds. Herit. Sci. **3**, 4 (2015). https://doi.org/10.1186/s40494-015-0033-6
78. L. Vigorelli, A. Re, P. Buscaglia, N. Manfredda, M. Nervo, T. Cavaleri, P. Del Vesco, M. Borla, S. Grassini, L. Guidorzi et al., Comparison of two ancient Egyptian Middle Kingdom statuettes from the Museo Egizio of Torino through computed tomographic measurements. J. Archaeol. Sci. Rep. **44**, 103518 (2022). https://doi.org/10.1016/j.jasrep.2022.103518
79. L. Vigorelli, A. Re, L. Guidorzi, T. Cavaleri, P. Buscaglia, M. Nervo, F. Facchetti, M. Borla, S. Grassini, A. LoGiudice, X-ray imaging investigation on the gilding technique of an ancient Egyptian Taweret wooden statuette. J. Imaging (2021). https://doi.org/10.3390/jimaging7110229
80. L. Vigorelli, A. Re, L. Guidorzi, R. Brancaccio, C. Bortolin, N. Grassi, G. Mila, N. Pastrone, R. Sacchi, S. Grassini et al., The study of ancient archaeological finds through X-ray tomography: the case of the "Tintinnabulum" from the Museum of Anthropology and Ethnography of Torino. J. Phys. Conf. Ser. **2204**, 012034 (2022). https://doi.org/10.1088/1742-6596/2204/1/012034
81. L. Vigorelli, E. Croce, D. Angelici, R. Navone, S. Grassini, L. Guidorzi, A. Re, A. Lo Giudice, X-ray micro-tomography as a method to distinguish and characterize natural and cultivated pearls. Condens. Matter (2021). https://doi.org/10.3390/condmat6040051
82. D. Nykonenko, O. Yatsuk, L. Guidorzi, A. Lo Giudice, F. Tansella, L.P. Cesareo, G. Sorrentino, P. Davit, M. Gulmini, A. Re, Glass beads from a Scythian grave on the island of Khortytsia (Zaporizhzhia, Ukraine): insights into bead making through 3D imaging. Herit. Sci. **11**, 238 (2023). https://doi.org/10.1186/s40494-023-01078-0
83. H. Alarashi, M. Benz, J. Gresky, A. Burkhardt, A. Fischer, L. Gourichon, M. Gerlitzki, M. Manfred, J. Sakalauskaite, B. Demarchi et al., Threads of memory: reviving the ornament of a dead child at the Neolithic village of Ba'ja (Jordan). PLoS ONE **18**, e0288075 (2023). https://doi.org/10.1371/journal.pone.0288075
84. F. Tansella, L. Vigorelli, G. Ricchiardi, A. Re, L. Bonizzoni, S. Grassini, M. Staropoli, A. Lo Giudice, X-ray computed tomography analysis of historical woodwind instruments of the late eighteenth century. J. Imaging (2022). https://doi.org/10.3390/jimaging8100260
85. E.H. Lehmann, E. Deschler-erb, A. Ford, Neutron tomography as a valuable tool for the non-destructive analysis of historical bronze sculptures. Archaeometry **52**, 272–285 (2010). https://doi.org/10.1111/j.1475-4754.2009.00480.x
86. N. Kardjilov, I. Manke, A. Hilger, M. Strobl, J. Banhart, Neutron imaging in materials science. Mater. Today **14**, 248–256 (2011). https://doi.org/10.1016/S1369-7021(11)70139-0
87. E. Lehmann, D. Mannes, A. Kaestner, C. Grünzweig, Recent applications of neutron imaging methods. Phys. Procedia **88**, 5–12 (2017). https://doi.org/10.1016/j.phpro.2017.06.055
88. F. Salvemini, A. Williams, D. Edge, B. Schillinger, F. Cantini, F. Grazzi, On the use of neutron imaging methods to identify microstructural features in ancient Indian swords and armour. Microchem. J. **159**, 105397 (2020). https://doi.org/10.1016/j.microc.2020.105397
89. N. Gelli, L. Giuntini, F. Cantini, O. Sans-Planell, M. Magalini, M. Manetti, L. Sodi, M. Massi, L. Castelli, C. Czelusniak et al., The new INFN-CHNet neutron imaging facility. Nucl. Instrum. Methods Phys. Res. Sect. A **1051**, 168189 (2023). https://doi.org/10.1016/j.nima.2023.168189

90. F. Salvemini, V. Luzin, F. Grazzi, S. Olsen, K. Sheedy, S. Gatenby, M.-J. Kim, U. Garbe, Archaeometric investigations on manufacturing processes in ancient cultures with the neutron imaging station DINGO at ANSTO. Phys. Procedia **88**, 116–122 (2017). https://doi.org/10.1016/j.phpro.2017.06.015
91. F. Grazzi, F. Cantini, F. Salvemini, A. Scherillo, B. Schillinger, A. Kaestner, D. Edge, A. Williams, The investigation of Indian and central Asian swords through neutron methods. J. Archaeol. Sci. Rep. **20**, 834–842 (2018). https://doi.org/10.1016/j.jasrep.2018.06.010
92. F. Cantini, S. Creange, Y. Li, L. van Eijck, N. Kardjilov, S. Kabra, F. Grazzi, Morphological and microstructural characterization of an ancient Chola bronze statuette by neutron based non-invasive techniques. Archaeol. Anthropol. Sci. (2023). https://doi.org/10.21203/rs.3.rs-3706226/v1
93. F. Cantini, A. Scherillo, A. Fedrigo, M. Galeotti, A. Cagnini, S. Porcinai, A. Patera, F. Morandini, F. Grazzi, The Vittoria Alata from Brescia: a combined neutron techniques and SEM-EDS approach to the study of the alloy of a bronze Roman statue. J. Archaeol. Sci. Rep. **51**, 104112 (2023). https://doi.org/10.1016/j.jasrep.2023.104112
94. R. Van Langh, E. Lehmann, S. Hartmann, A. Kaestner, F. Scholten, The study of bronze statuettes with the help of neutron-imaging techniques. Anal. Bioanal. Chem. **395**, 1949–1959 (2009). https://doi.org/10.1007/s00216-009-3058-4
95. F. Grazzi, F. Cantini, N. Gelli, The new NICHE imaging station at the TRIGA-Reactor in Pavia. https://www.isnr.de/images/NR-Newsletter/nr17.pdf. Accessed 30 May 2024
96. F. Grazzi, F. Cantini, O. Sans-Planell, M. Magalini, L. Vigorelli, G. Marcucci, M. Clemenza, M. Morigi, A. Re, D. Alloni et al., A work-horse neutron imaging station at the Laboratorio Energia Nucleare Applicata (LENA) in Pavia (Italy): instrumental components and applications in the frame of the CHNet-NICHE INFN experiment. J. Phys. Conf. Ser. **2605**, 012006 (2023). https://doi.org/10.1088/1742-6596/2605/1/012006
97. O. Sans-Planell, F. Cantini, M. Costa, E. Durisi, F. Grazzi, E. Mafucci, V. Monti, R. Bedogni, Y. Li, Improved methodologies to study the performance of the ANET Compact Neutron Collimator. Nucl. Instrum. Methods Phys. Res. Sect. A **1052**, 168260 (2023). https://doi.org/10.1016/j.nima.2023.168260
98. Start of Measurement Series: Fraunhofer IIS and Staatliche Museen zu Berlin Digitize Benin Bronzes Using High Energy Computed To-mography. https://www.smb.museum/en/whats-new/detail/start-of-measurement-series-fraunhofer-iis-and-staatliche-museen-zu-berlin-digitize-benin-bronzes-using-high-energy-computed-to-mography/. Accessed 14 Apr 2024
99. T. Kleynhans, C.M. Schmidt Patterson, K.A. Dooley, D.W. Messinger, J.K. Delaney, An alternative approach to mapping pigments in paintings with hyperspectral reflectance image cubes using artificial intelligence. Herit. Sci. **8**, 84 (2020). https://doi.org/10.1186/s40494-020-00427-7
100. G.A. Licciardi, F. Del Frate, Pixel unmixing in hyperspectral data by means of neural networks. IEEE Trans. Geosci. Remote Sens. **49**, 4163–4172 (2011). https://doi.org/10.1109/TGRS.2011.2160950
101. X. Zhang, Y. Sun, J. Zhang, P. Wu, L. Jiao, Hyperspectral unmixing via deep convolutional neural networks. IEEE Geosci. Remote Sens. Lett. **15**, 1755–1759 (2018)
102. M. Wang, M. Zhao, J. Chen, S. Rahardja, Nonlinear unmixing of hyperspectral data via deep autoencoder networks. IEEE Geosci. Remote Sens. Lett. **16**, 1467–1471 (2019). https://doi.org/10.1109/LGRS.2019.2900733
103. S. Kogou, L. Lee, G. Shahtahmassebi, H. Liang, A new approach to the interpretation of XRF spectral imaging data using neural networks. X-Ray Spectrom. **50**, 310–319 (2021). https://doi.org/10.1002/xrs.3188
104. M. Vermeulen, A. McGeachy, B. Xu, H. Chopp, A. Katsaggelos, R. Meyers, M. Alfeld, M. Walton, XRFast a new software package for processing of MA-XRF datasets using machine learning. J. Anal. At. Spectrom. **37**, 2130–2143 (2022). https://doi.org/10.1039/D2JA00114D
105. C. Jones, N.S. Daly, C. Higgitt, M.R.D. Rodrigues, Neural network-based classification of X-ray fluorescence spectra of artists' pigments: an approach leveraging a synthetic dataset created using the fundamental parameters method. Herit. Sci. **10**, 88 (2022). https://doi.org/10.1186/s40494-022-00716-3
106. A. Bombini, L. Anderlini, L. dell'Agnello, F. Giacomini, C. Ruberto, F. Taccetti, Hyperparameter optimisation of Artificial Intelligence for Digital REStoration of Cultural Heritages (AIRES-CH) models, in *Proceedings of the Computational Science and Its Applications—ICCSA 2022 Workshops, Cham, 2022* (2022), pp. 91–106
107. A. Bombini, F.G.-A. Bofías, C. Ruberto, F. Taccetti, A cloud-native application for digital restoration of cultural heritage using nuclear imaging: THESPIAN-XRF. Rendiconti Lincei. Scienze Fisiche e Naturali **34**, 867–887 (2023)
108. L. Liu, T. Miteva, G. Delnevo, S. Mirri, P. Walter, L. de Viguerie, E. Pouyet, Neural networks for hyperspectral imaging of historical paintings: a practical review. Sensors **23**, 2419 (2023). https://doi.org/10.3390/s23052419
109. M. Fiorucci, M. Khoroshiltseva, M. Pontil, A. Traviglia, A. Del Bue, S. James, Machine learning for cultural heritage: a survey. Pattern Recogn. Lett. **133**, 102–108 (2020). https://doi.org/10.1016/j.patrec.2020.02.017